

SURFACE AND DEEPWATER DISSOLVED INORGANIC CARBON AND pH IN THE NORTHERN GULF OF MEXICO

A Thesis

by

JORDAN WAYNE YOUNG

Submitted to the Office of Graduate and Professional Studies of
Texas A&M University
in partial fulfillment of the requirements for the degree of

MASTER OF SCIENCE

Chair of Committee,
Committee Members,

Head of Department,

Shari Yvon-Lewis
Katie Shamberger
Piers Chapman
Niall Slowey
Ethan Grossman
Debbie Thomas

August 2016

Major Subject: Oceanography

Copyright 2016 Jordan Wayne Young

ABSTRACT

The Gulf of Mexico is known for its numerous natural seeps as well as a very active drilling program for the oil located in its sediments. This study examines water column in an active drilling and seep region in two different years, assessing the carbonate system chemistry in the deep northern Gulf of Mexico waters. There were two summer cruises in the Northern Gulf of Mexico two years apart, 2012 and 2014. Over 350 samples were collected for DIC and TA measurements on the first cruise and 115 samples were collected on the second cruise. The remaining carbon system parameters, such as pH and $p\text{CO}_2$, were determined for each sample. The cruises were compared to GOMECC cruises in nearby region and showed that surface DIC was statistically more variable for this sample region but surface TA was not as statistically variable, suggesting a larger biological activity gradient than in the GOMECC cruises. The Mississippi River plume extended into the sampling areas on both cruises but to different extents and directions, likely due to the 227% increased discharge rate between the two years. Saturation states of calcite and aragonite approach an average of one only in the densest water sampled, suggesting favorable values for calcite and aragonite structure builders. The deepwater in the northern Gulf of Mexico was statistically significant to similar density water in the Atlantic, suggesting that the deepwater has returned to pre spill conditions, according to the carbonate chemistry.

ACKNOWLEDGEMENTS

I would like to thank Dr. Shari Yvon-Lewis, my advisor, for allowing me to complete this research and providing her extremely helpful experience and input throughout the way. I would also like acknowledge the rest of my committee, Dr. Katie Shamberger, Dr. Piers Chapman, Dr. Niall Slowey, and Dr. Ethan Grossman.

Secondly, I would like to thank multiple others for helping me in the lab. I thank Rachel Reddig for her early sample running help and company into the late hours of the night watching titrations. I thank Reagan Errera for helping me understand the fine tuning of the machine and for all the incredibly useful information on how to deal with the calculations in a more manageable fashion. I want to thank Connie Previti for helping tremendously in the sample running and general lab upkeep. She provided countless hours and made the lab much more enjoyable in the long days.

NOMENCLATURE

DIC	Dissolved Inorganic Carbon
TA	Total Alkalinity
GISR	Gulf Integrated Spill Research Consortium
LUMCON	Louisiana Universities Marine Consortium
$p\text{CO}_{2(a)}$	Partial Pressure of Carbon Dioxide in Air
$p\text{CO}_{2(w)}$	Partial Pressure of Carbon Dioxide in Seawater
Ω_{CA}	Calcite Saturation State
Ω_{ARG}	Aragonite Saturation State
GOM	Gulf of Mexico
G01	GISR Cruise Number 1
G06	GISR Cruise Number 6
CRM	Certified Reference Material

TABLE OF CONTENTS

	Page
ABSTRACT	ii
ACKNOWLEDGEMENTS	iii
NOMENCLATURE	iv
TABLE OF CONTENTS	v
LIST OF FIGURES	vii
LIST OF TABLES	viii
1. INTRODUCTION	1
1.1 Background.....	3
1.2 Objectives.....	6
1.3 Hypotheses.....	6
2. METHODS AND MATERIALS	7
2.1 Sample Bottle Preparation and Collection	7
2.2 Cruise Overview	8
2.3 Sample Analysis	10
2.3.1 Dissolved Inorganic Carbon	10
2.3.2 Total Alkalinity.....	11
2.3.3 Reagents and Buffers	11
2.3.4 Calculations	12
2.3.5 Salinity and Temperature	13
2.3.6 Continuous Surface Water and Air pCO ₂ Measurements	14

3. RESULTS	16
3.1 Surface Results	16
3.2 Profile Results.....	31
4. DISCUSSION	35
5. CONCLUSIONS AND FUTURE WORK.....	45
5.1 Conclusions.....	45
5.2 Future Work	47
REFERENCES	49

LIST OF FIGURES

FIGURE	Page
1 G01 Station Map.....	9
2 G06 Station Map.....	9
3 G01 Surface Temperature	17
4 G01 Surface Salinity.....	17
5 G06 Surface Temperature	18
6 G06 Surface Salinity.....	18
7 G01 Surface $p\text{CO}_{2(\text{W})}$	19
8 G01 Surface $p\text{CO}_{2(\text{A})}$	20
9 G06 Surface $p\text{CO}_{2(\text{W})}$	20
10 G06 Surface $p\text{CO}_{2(\text{A})}$	21
11 G01 Fluorescence	22
12 G06 Fluorescence	22
13 G01 Surface DIC.....	23
14 G06 Surface DIC.....	24
15 G01 Surface TA	25
16 G06 Surface TA	25
17 G01 Surface Ω_{CA}	26
18 G01 Surface Ω_{ARG}	27

19	G06 Surface Ω_{CA}	27
20	G06 Surface Ω_{ARG}	28
21	G01 Surface Characteristics.....	29
22	G06 Surface Temperature and Salinity	30
23	Normalized TA	32
24	Normalized DIC.....	33
25	CLIVAR Cruise Lines	33
26	Saturation States	34
27	Geostrophic Flows during G01 Cruise	36
28	Geostrophic Flows during G06 Cruise	36
29	GOMECC2 Cruise Stations	40
30	GISR versus GOMECC TA Comparison	42
31	GISR versus GOMECC DIC Comparison	43

1. INTRODUCTION

As fossil fuel combustion continues to increase with increasing population, atmospheric CO₂ levels are steadily increasing and surpassing the highest previously recorded measurements. The ocean acts as a sink for approximately 30% of the total anthropogenically emitted CO₂, with fossil fuel combustion providing the majority of this addition [Le Quéré, 2010; Tans, 2009]. This anthropogenically emitted CO₂ (and general atmospheric CO₂), as well as CO₂ respired through breakdown of oils and other organic matter from within the water column, react with seawater to form carbonic acid (H₂CO₃) which easily dissociates to bicarbonate (HCO₃⁻):



The introduced acidity from the free H⁺ ion is then buffered with carbonate (CO₃⁻²) to form bicarbonate:



This dissolved CO₂ (dissolved pCO₂) affects the carbonate system by adding more H⁺ ion (equation 1) into the world's oceans leading to a decrease in overall pH, hence the term Ocean Acidification. As the acidity in the ocean increases it begins to dissolve the calcium carbonate structures that many organisms, such as corals and

oysters, use to create their skeletons and shells [Orr *et al* 2005]. Since the industrial revolution, ocean pH has dropped 0.1 units and is expected to drop an additional 0.3 units by the end of the century if increases in atmospheric concentration of CO₂ remain as is [Caldeira and Wickett, 2005].

Ocean acidification can be quantified by calculating the pH of the water through measurements of the carbonate system. A minimum of two of the following parameters are needed for this calculation; dissolved inorganic carbon (DIC), total alkalinity (TA), and partial pressure of carbon dioxide (pCO_{2(aq)}). DIC is defined as the sum of the concentrations of the inorganic carbon containing molecules dissolved in seawater:

$$\text{DIC} = [\text{CO}_2] + [\text{H}_2\text{CO}_3] + [\text{HCO}_3^-] + [\text{CO}_3^{2-}] \quad (3)$$

The TA is defined as:

$$\text{TA} = [\text{HCO}_3^-] + 2[\text{CO}_3^{2-}] + [\text{B(OH)}_4^-] + [\text{OH}^-] + [\text{HPO}_4^{2-}] + 2[\text{PO}_4^{3-}] + [\text{SiO(OH)}_3^-] + [\text{NH}_3] + [\text{HS}^-] \dots - [\text{H}^+]_{\text{free}} - [\text{HSO}_4^-] - [\text{HF}] - [\text{H}_3\text{PO}_4] - \dots \quad (4)$$

The main three components contributing to total alkalinity are the [HCO₃⁻], 2[CO₃²⁻], and [B(OH)₄⁻]. The hydroxide (OH⁻), phosphates (HPO₄²⁻ and PO₄³⁻), silicate (SiO(OH)₃⁻), ammonia (NH₃), and hydrogen sulfide (HS⁻) also contribute to TA, albeit much less. The ellipses represent other acids and bases that are too small to measure or are in small

enough concentration to not make a large difference in the measurement [Dickson *et al.*, 2007].

Both DIC and TA can vary naturally in many ways in the water column. DIC decreases in surface waters via photosynthesis as the removal of CO₂ is integral to the phytoplankton organic matter production. On the other hand, DIC in the water column increases during bacterial oxidation of organic matter, as CO₂ is added to the water as a byproduct of respiration. TA concentrations will not change during photosynthesis or respiration but will be affected by water mass mixing, precipitation, and evaporation. Thus, TA is a conservative property of water and can be used to trace water mass movement. Calcium carbonate dissolution and formation do have an effect on both DIC and TA, with dissolution causing an increase in both properties and formation causing a decrease in both properties.

1.1 Background

The northern Gulf of Mexico is a very important region for the economy of the surrounding Gulf States. In 2010, the commercial fisheries of the five Gulf States brought in approximately \$639 million dollars through shellfish, oysters and mollusks, and larger more recreational fishing [EPA General Facts, 2012]. The Gulf of Mexico is also home to numerous coral reefs, such as the Flower Gardens National Bank off the coast of Texas. These organisms utilize carbonate ions in the surrounding seawater to create their shells or coralline structures. As pH decreases, the carbonate ion

concentrations decrease as well. A way to track these ion concentrations is defined as calcite saturation state (Ω_{CA}) and aragonite saturation state (Ω_{ARG}) where $\Omega = \frac{[\text{Ca}^{2+}][\text{CO}_3^{2-}]}{K_{\text{sp}}}$ and the defining difference between calcite and aragonite being their respective solubility constant [Doney *et al* 2009].

The Gulf of Mexico also contains an important oil industry with many established rigs and pipelines. As technology advances the ability to retrieve oil from much deeper water, these areas are becoming more important to understand. Oil spills are bound to happen given the amount of oil the area produces along with the structures built to extract it. There are also large inputs of hydrocarbons via natural seeps in these waters, roughly 600,000 metric tons per year with a large variability [Kvenvolden and Cooper 2003]. Spills and accidents, such as the Deep Water Horizon incident, can also add large amounts of hydrocarbons to the deep waters. This oil, along with other hydrocarbons, provides a source of deep water carbon for bacterial respiration. As stated earlier, respired CO_2 leads to increased DIC and decreased pH. Deep water organisms have been found to show sensitivity to CO_2 concentration increases and the associated pH decreases [Seibel and Walsh, 2001].

The Gulf of Mexico is a characteristically special region of study in terms of ocean acidification. The Gulf of Mexico is a very deep basin with restricted entry and exit points for its water flow. There are not high latitude cold points to increase the density of its surface waters and create new deepwater or directly establish a current.

On the surface, the Gulf of Mexico has what is known as the Loop Current, which is characterized by water entering the gulf in the Yucatan Strait making a loop before exiting the Florida Strait and going on to form the Gulf stream. This surface current is present year round but changes in magnitude and proximity to the gulf states. Eddies are also known to break off the loop current and travel across the gulf. These eddies change the sea surface height and thus the currents and water movement at the surface. The deep water circulation of the Gulf of Mexico is much different than the surface currents. With the Yucatan and Florida straits forming a lip on the edge of the gulf, the sill heights dictate how deep water flows into and out of the gulf. Due to the relatively shallow depth of the Florida strait (~800m) most of the deep water cannot enter or exit through that region. Thus deepwater enters the gulf from the Caribbean Sea over the Yucatan strait sill at depths 2000m and greater. The deepwater also has to exit in this same region, which leads to side by side entry and exit of the gulf deepwater [Nowlin *et al* 2001].

Another very special aspect of the Gulf of Mexico is the amount of riverine fresh water. The Mississippi River and Atchafalaya River both empty into the northern Gulf of Mexico and can impact the characteristics of the surface water in this region. These rivers bring with them freshwater which overlays the more dense saltwater and can act as a lens of stratification. High levels of nutrients, DIC, and TA are also brought with this freshwater. These high values, coupled with the low salinity, lead to high

saturation states of both calcite and aragonite in the northern Gulf of Mexico [Wanninkhof *et al* 2015; Wang *et al* 2013]. In addition, the lens can also heavily stratify the water column and create a seasonal area of low oxygen commonly referred to as the “Dead Zone”; however this area tends to run along the shelf of the Louisiana and Texas border and not the entire gulf.

1.2 Objectives

The objective of this research is to assess the dissolved inorganic carbon, total alkalinity, and pH in the deep waters of Northern Gulf of Mexico. In addition, the study will investigate any changes in these parameters over a 2 year period at select stations and in the surface waters.

1.3 Hypothesis

The hypotheses that steer this research are as follows:

1. Northern Gulf of Mexico surface waters will show evidence of increased DIC, TA, Ω_{CA} , and Ω_{ARG} due to Mississippi River Influence.
2. Deep water in the Northern Gulf of Mexico will have similar DIC and TA concentrations in comparison to water of the same density in the deep Atlantic Ocean.

2 MATERIALS AND METHODS

2.1 Sample Bottle Preparation and Collection

Sample containers consisted of two sizes of borosilicate bottles (Corning Glass) 350 ml and 500 ml. Bottles were washed using a diluted soap made from deionized water and Alconox. The bottles were then rinsed 3-4 times using deionized water to remove all soap. After rinsing, bottles were placed in an acid bath (3 L of 6N hydrochloric acid diluted with 27 L of deionized water) for a minimum of 12 hours. Another rinse cycle of about 3-4 times with purified low total organic carbon (TOC) water (Barnstead Nanopure) removed any residual acid on the bottles before they were placed in a combustion oven to combust at 500 °C for a minimum of six hours. Combusted bottles were covered with aluminum foil that was also combusted.

Samples collected for DIC and TA were collected from a rosette with Niskin bottles. Samples were collected immediately after oxygen samples were drawn from each Niskin, in turn, using a tube to connect to the nipple for minimizing air interaction. Bottles were rinsed with sample water roughly three times the bottle volume before stopping flow. A small volume of headspace was left to allow water expansion without compromising airtight integrity. Samples were poisoned with 50 µl or 100 µl of saturated mercuric chloride solution for 350 ml and 500 ml bottles, respectively. This poison addition was to halt all biological activity in the samples until analysis. Samples

were then sealed with a glass stopper coated lightly in silicone grease and held down tight with industrial rubber bands and a zip tie to hold everything in place. The samples were then placed in a dark and cool location aboard the ship in metal crates. Upon returning to Texas A&M University, the samples were transferred to a refrigerated room until analysis.

2.2 Cruise Overview

Water samples were collected throughout the water column around the Deepwater Horizon Accident site (DWH) in the Northern Gulf of Mexico (NGOM) (Figure 1). The samples were collected for DIC and TA analysis on two separate cruises on the Research Vessel Pelican operated by Louisiana Universities Marine Consortium (LUMCON). The two cruises are a subset of the cruises conducted for the Gulf Integrated Spill Research (GISR) Consortium. Two cruises were completed, both departing and returning to the LUMCON port in Chauvin, Louisiana. The first cruise, GISR 01 (G01), occurred from 7/5/2012 to 7/11/2012 and was composed of 30 stations where 338 samples were collected (Figure 1). The second cruise, GISR 06 (G06), took place between 6/24/2014 and 7/2/2014 in the same location (Figure 2). However, only 10 stations were sampled for DIC and TA with 115 samples collected. Stations on this cruise were chosen to try to cover the largest spatial area possible that overlapped with GISR 01. Both cruises covered an area of roughly 1360 km² located around the Deepwater Horizon catastrophe site.

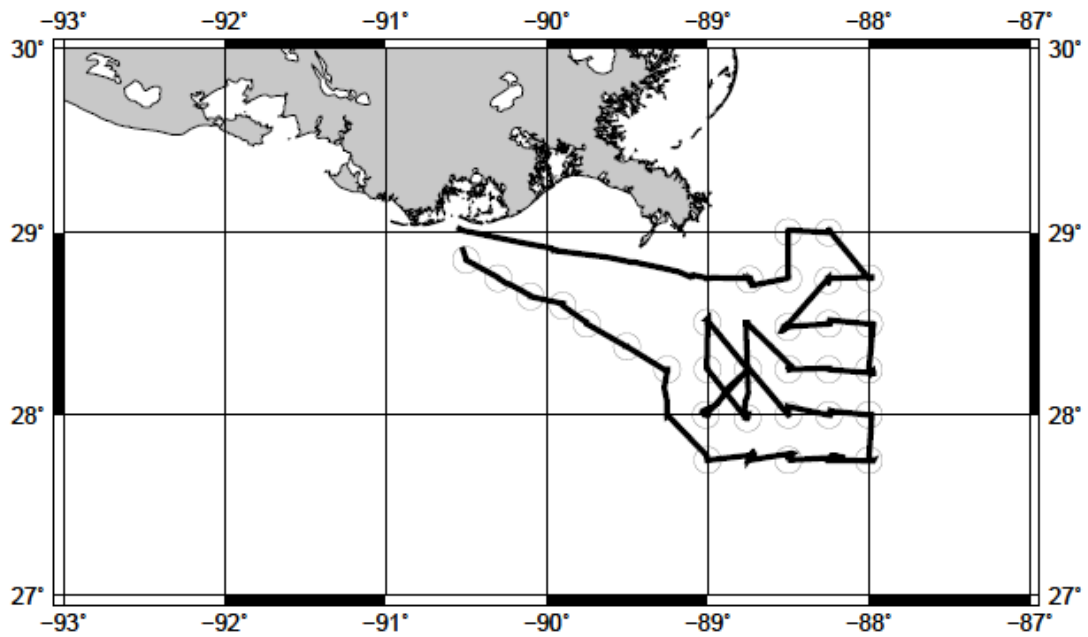


Figure 1. G01 Station map. The black line represents the cruise track of the ship and the circles represent where CTD's were deployed on stations.

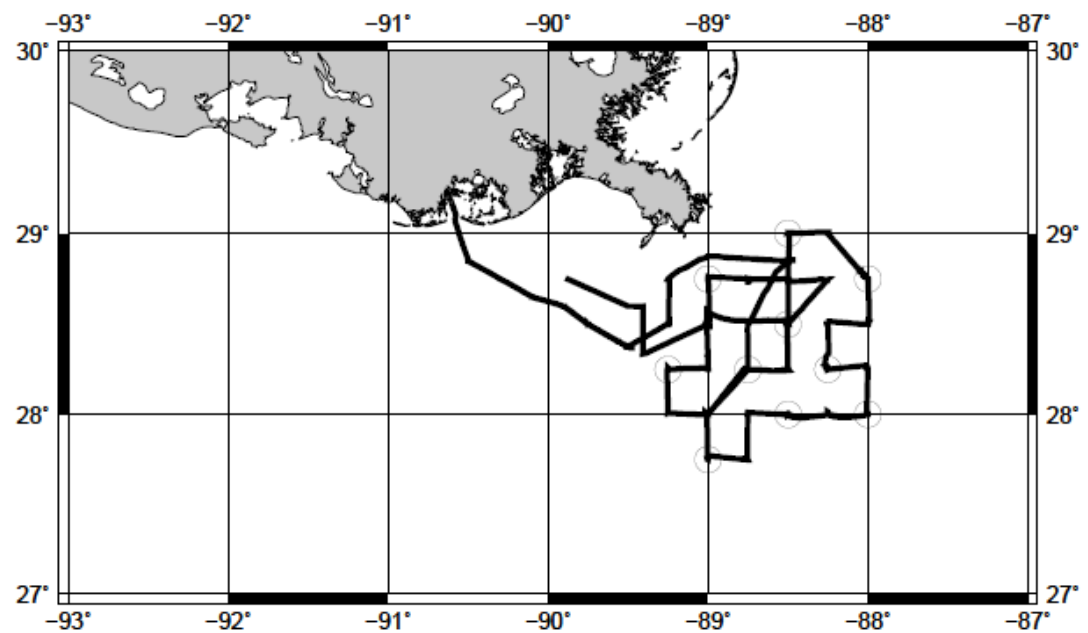


Figure 2. G06 Station map. The black line represents the cruise track of the ship and the circles represent where CTD's were deployed on stations.

2.3 Sample Analysis

2.3.1 Dissolved Inorganic Carbon

DIC was measured using a VINDTA (Versatile Instrument for the Determination of Total inorganic carbon and Alkalinity, MARIANDA, Germany) and a coulometer (CM5015, UIC, Inc, USA). The method followed is described in SOP 2 [Dickson *et al.*, 2007] and was completed using certified reference material (CRM) obtained from Dr. Andrew Dickson at Scripps Institution of Oceanography in La Jolla, California, USA. Precision of analysis was measured on a day to day basis and averaged 0.4% error (8 $\mu\text{mol/kg}$) for GISR 01 and 0.3% (6 $\mu\text{mol/kg}$) for GISR 06.

This coulometric technique measures DIC by titrating a fixed volume of sample with phosphoric acid to shift all the carbonate system species to CO_2 . The resultant CO_2 is then stripped from the water sample using an ultra high purity nitrogen carrier gas that has been cleaned with Ascarite II (Sigma Aldrich). The gas passes through silica gel and magnesium perchlorate to remove any water from the stream and a silica packed Orbo tube (Supelco Orbo 53) to remove any excess phosphoric acid before it reaches the coulometer cell. The coulometer cell becomes more transparent through addition of CO_2 which is detected via a lamp shining through the cell into a photodiode. The coulometer then uses a measured amount of electricity to energize the cell and return it to a known level of transparency; the energy used is given as counts.

Dissolved inorganic carbon can be calculated using these counts via the equation given in the standard operating procedures found in SOP 2 [Dickson *et al.*, 2007].

2.3.2 Total Alkalinity

TA is measured using a Gran titration and the open cell method described in SOP 3b [Dickson *et al.*, 2007]. The same certified reference materials used for the DIC are used for the alkalinity samples. Open cell titration is a method that uses a known volume of sample and monitors the pH change with multiple additions of known volumes of hydrochloric acid. The process begins with an initial addition of acid to reduce the sample pH to 3.5-4 units. Then smaller quantities are added incrementally to bring the pH down to 3.0. Throughout the analysis the EMF (electromotive response) is monitored using a double junction electrode (Metrohm). The alkalinity is then calculated from the outputs of this titration using the procedures documented in SOP 3b [Dickson *et al.*, 2007] bulk calculations for alkalinity were completed using a MATLAB script created by Dr. C. Sabine at National Oceanic and Atmospheric Administration-Pacific Marine Environmental Laboratory (NOAA/PMEL) which follows the same procedures mentioned previously in SOP 3b.

2.3.3 Reagents and Buffers

In order to accurately measure the TA (which was estimated to be around 2000 $\mu\text{mol/kg}$) with a 10 ml burette of titrant while using a 100 ml open titration cell, the acid titrant used had a concentration of 0.025 N HCl. The electrode probe (Metrohm)

used a 3 M KCl solution per instructions from Metrohm. The Double Junction reference probe used Orion's AgCl solutions for the inner and outer filling solutions.

The alkalinity titration required daily calibration with buffers of known pH. The two buffers used are Tris/Tris-HCl (Tris) and 2-Aminopyridine/Aminopyridine-HCl (AMP). Salts (NaCl, KCl, Na₂SO₄) are added to reach the correct ionic strength. The Tris and AMP are dried in a desiccator that is filled with phosphorus pentoxide to completely remove any excess water. The buffer solutions were made 2 liters at a time and were kept sealed in a dry dark cupboard.

2.3.4 Calculations

The parameters pH, pCO₂, and $\Omega_{\text{aragonite}}$ were calculated using the excel version of CO2SYS [Pierrot, 2006]. CO2SYS calculates the pH (in this case using the total scale) by using the input of DIC and TA, along with depth, temperature, salinity, and nutrients. The program also calculates the saturation states, although the value for the concentration of calcium is estimated using the salinity since calcium samples were not taken.

This assumes that Marcet's principle holds true for all water samples in the study, including those affected by the Mississippi river plume. The K_1 and K_2 constants chosen were from *Merbach et al.*, [1978] and refitted by *Dickson and Millero* [1987].

2.3.5 Salinity and Temperature

Salinity and temperature for each depth profile were measured continuously via the CTD (a rosette equipped to measure conductivity, temperature, and depth) at each station. Salinities were verified for accuracy with water samples from the CTD. These samples were taken only in the surface and bottom niskin bottles of the CTD. The salinity samples were analyzed at the Geophysical and Environmental Research Group (GERG) by Erik Quiroz.

2.3.6 Continuous Surface Water and Air pCO₂ Measurements

During G01 and G06, the ship was equipped with the ability to measure continuous pCO₂ for both the air and the surface seawater. The instrument used was built at Texas A&M University using a design modified from that of *Pierrot et al.* [2009] and based on the practices of *Takahashi* [1961]. A seawater intake located about 3 meters below the surface pumps in a water stream which is split before it reaches any bubble traps for other instruments. This surface seawater passes into a 1 L equilibrator via a spray nozzle allowing a larger surface area and thus faster equilibration of the headspace in the equilibrator. The flow of water is continuous. The headspace is constantly in contact with new surface water. The headspace is sampled by pumping out through a tube set above the spray nozzle to avoid any excess water. This sample is routed through a condenser and a Nafion dryer to remove water vapor before being analyzed. The outflow from the detector is sent back to the equilibrator to maintain the integrity of the recirculated headspace. The detectors used, an NDIR detector (LiCor 820) for G01 and a cavity ringdown spectrometer (Picarro) for G06, are non-destructive allowing the return flow into the headspace of the equilibrator. The equilibrator also had a second equilibrator in parallel with the same setup, where the headspace acted as a supply for the vent on the main equilibrator to allow the main sample chamber to run at ambient pressure without sucking in room air if the pressure

changed quickly. Atmospheric $p\text{CO}_2$ was also sampled by pumping in air at roughly 3.5 L min^{-1} through a line that ran along the vessel ending with the intake above the wheelhouse. This position was chosen to limit the exhaust from entering the sample. A cup-like device was also fitted onto the end and faced down to help avoid exhaust intake as well as rain or wave spray. The system automatically cycles between analyzing the equilibrator headspace and the atmospheric gas stream. The system was calibrated using gas cylinders with mixtures of known concentrations (Scott Gas, AirLiquide). A calibration curve was run once or twice, daily. It is important to note that during G06 there was a valve malfunction roughly halfway through the cruise, limiting the data obtained during that cruise.

3 RESULTS

3.1.1 Surface Results

Many different water characteristics were measured. Sea surface temperature peaked at 32°C during G01 near the northern stations located at -89°W 28.75°N and had a minimum of 28°C just east of the maximum (Figure 3). The salinity along the cruise track for G01 had a maximum of 37 PSU and a minimum of 21 PSU (Figure 4). G06 had a sea surface temperature maximum of 32 °C and a minimum of 25 °C, however this minimum was located in the bayou. The minimum located in the gulf was actually ~29°C (Figure 5). The salinity during cruise G06 ranged from a maximum of 37 PSU to a minimum of 19 PSU (Figure 6).

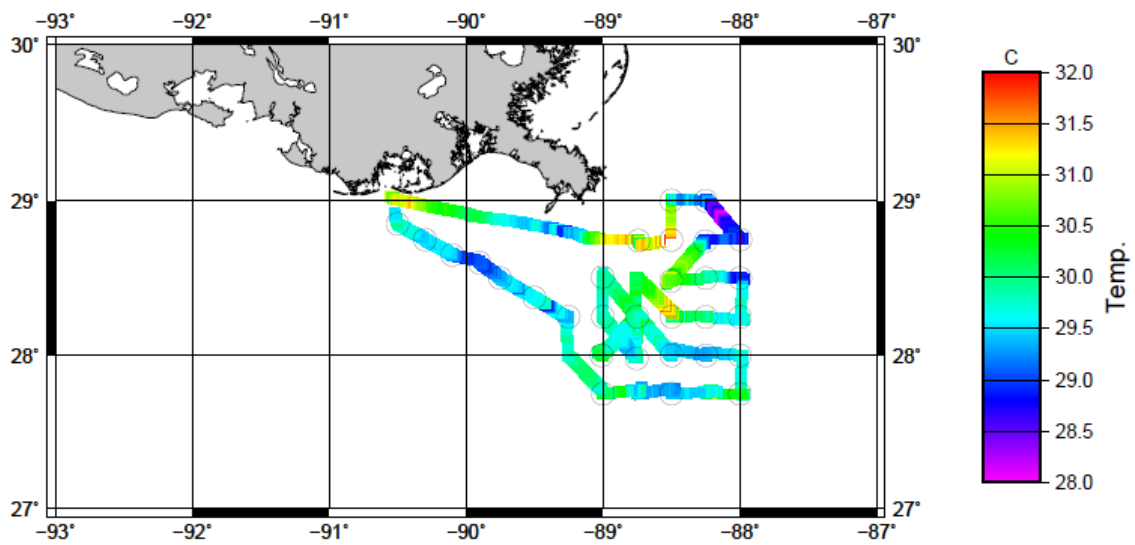


Figure 3. G01 Surface Temperature. Temperature in degrees C along cruise track.

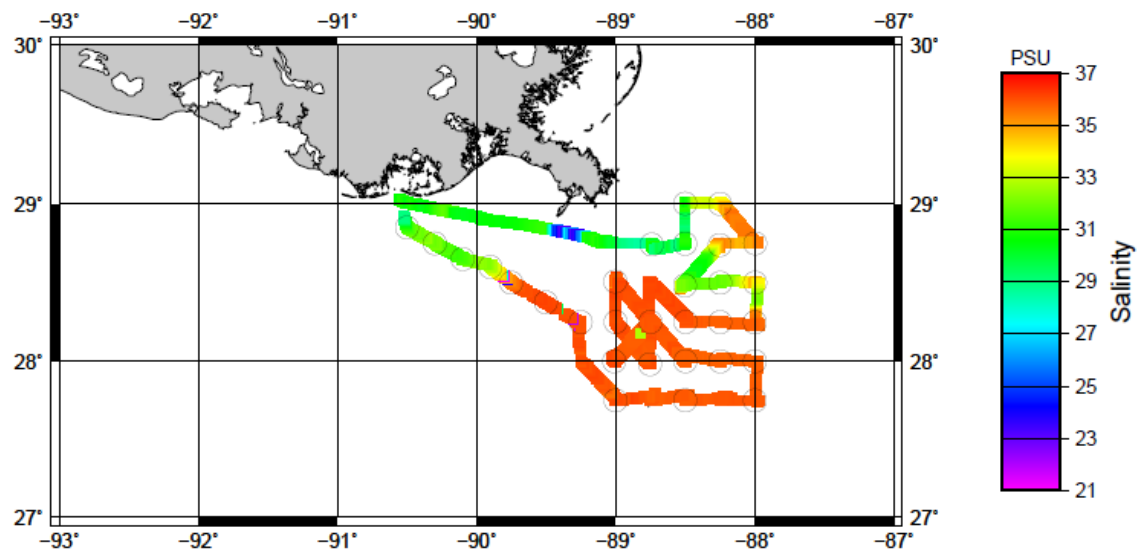


Figure 4. G01 Surface Salinity. Salinity in PSU's along cruise track.

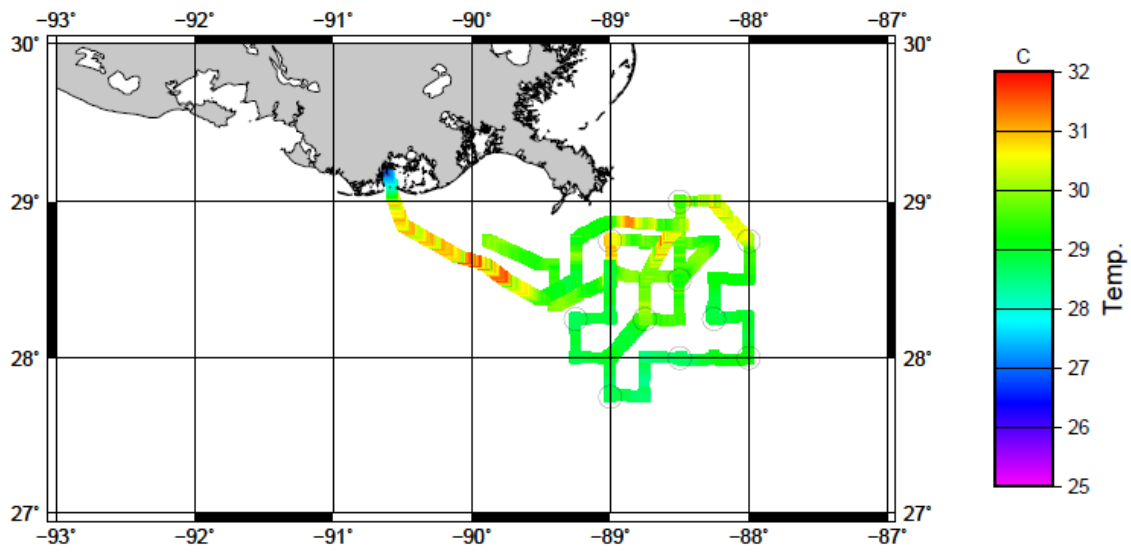


Figure 5. G06 Surface Temperature. Temperature in degrees C along cruise track.

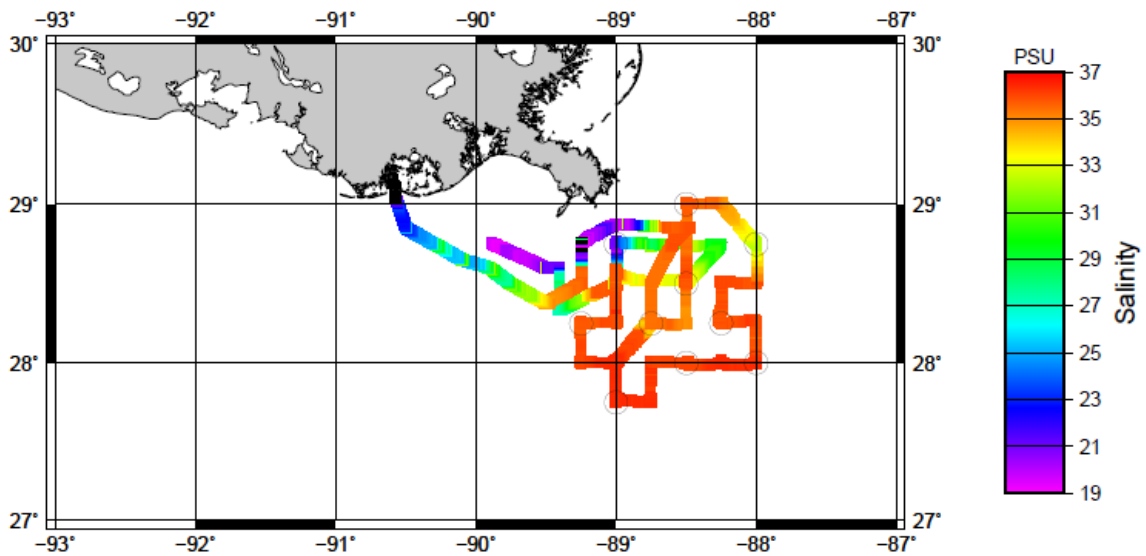


Figure 6. G06 Surface Salinity. Salinity in PSU's along cruise track.

Continuous shipboard measurements of $p\text{CO}_2$ for both air and surface water were measured for both cruises. G01 showed a range of $p\text{CO}_{2(w)}$ from 600ppm to 275ppm (Figure 7) and a $p\text{CO}_{2(a)}$ from 460ppm to 365ppm (Figure 8). G06, while only having a few days worth of data due to a valve malfunction, showed a much different story. The range of $p\text{CO}_{2(w)}$ went from a maximum of 1400ppm to a minimum of 130ppm (Figure 9). The $p\text{CO}_{2(a)}$ for G06 was similar to G01 in that the maximum was 465ppm and the minimum was 390ppm (Figure 10).

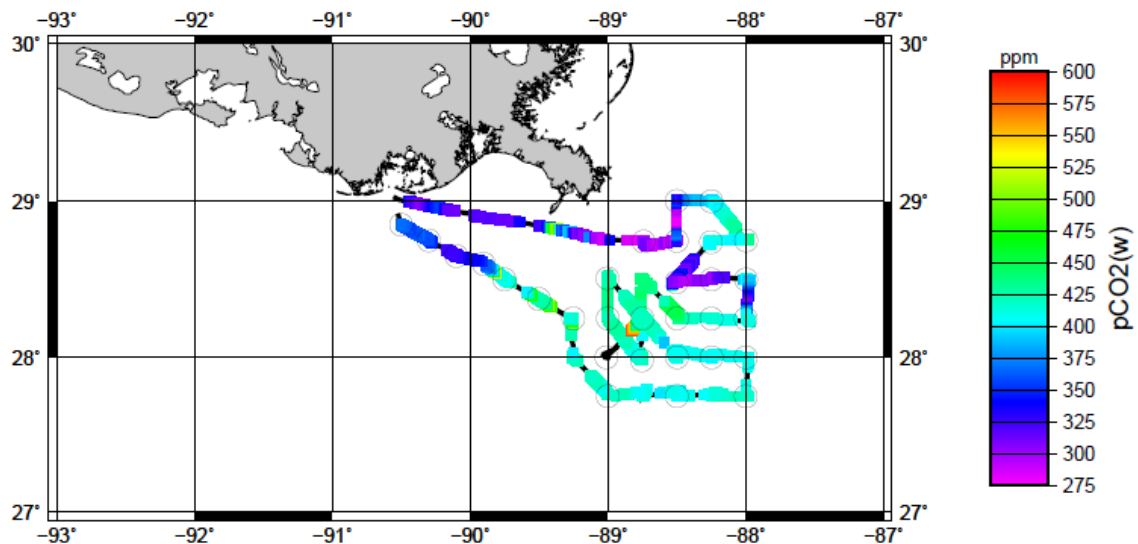


Figure 7. G01 Surface water $p\text{CO}_{2(w)}$. $p\text{CO}_{2(w)}$ in ppm along cruise track. Circles represent stations and black line in background represents cruise track.

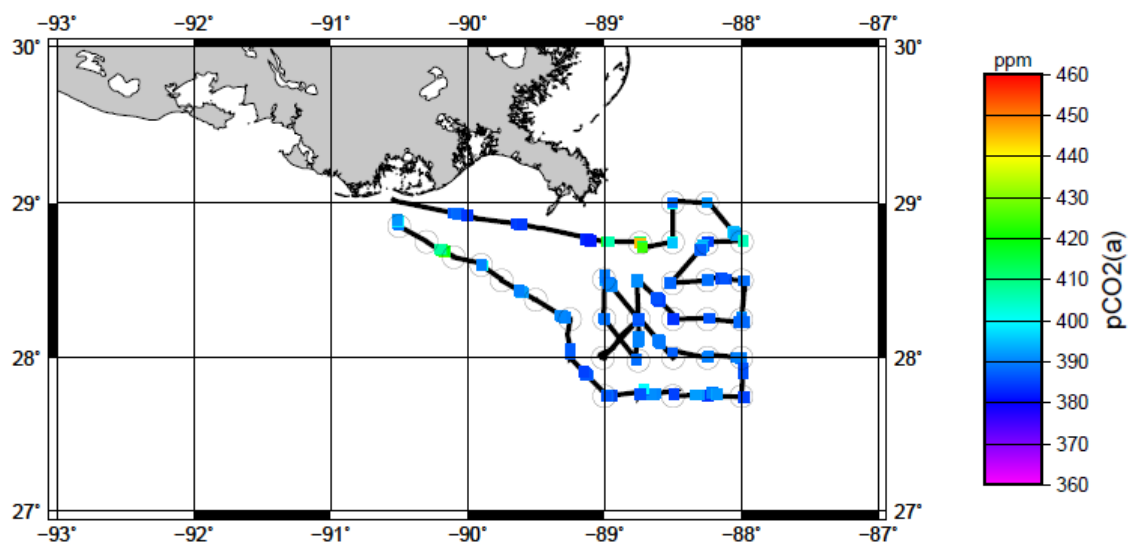


Figure 8. G01 Surface pCO_{2(a)}. pCO_{2(a)} in ppm along cruise track. Circles represent stations and black line in background represents cruise track.

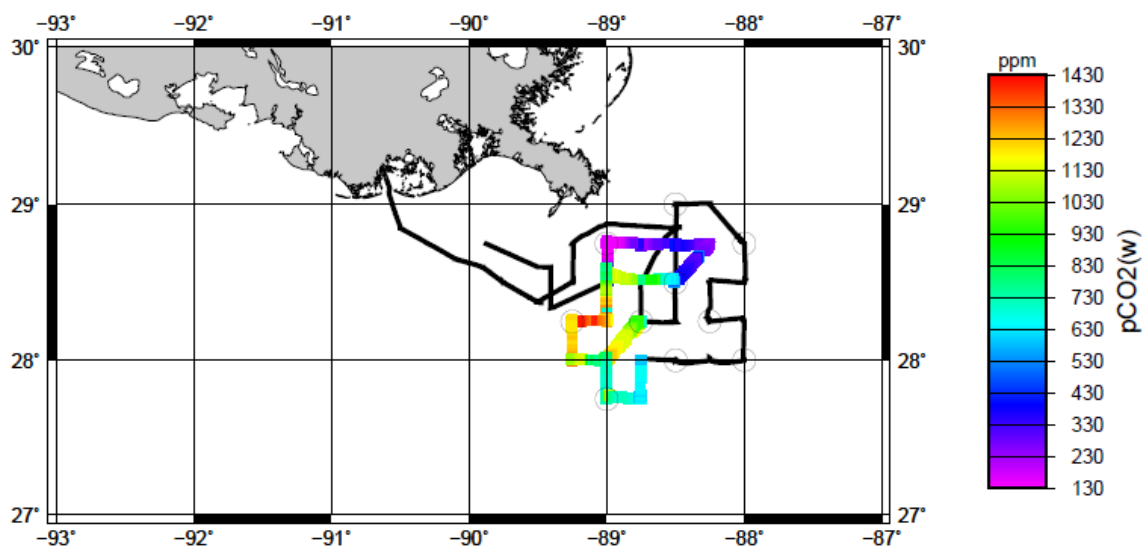


Figure 9. G06 Surface pCO_{2(w)}. pCO_{2(w)} in ppm along cruise track. Circles represent stations and black line in background represents cruise track.

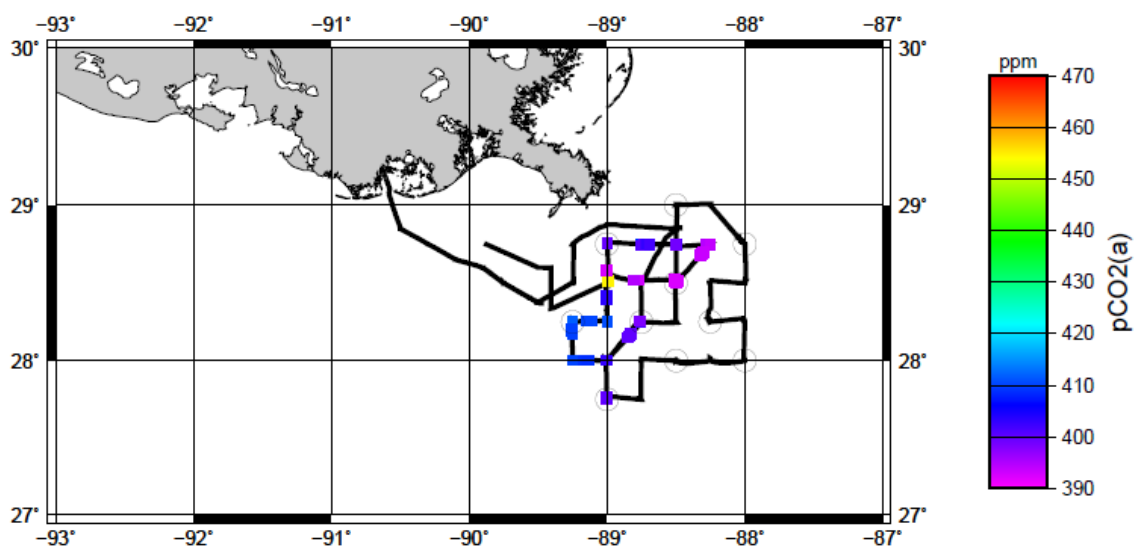


Figure 10. G06 Surface air pCO_{2(a)}. pCO_{2(a)} in ppm along cruise track. Circles represent stations and black line in background represents cruise track.

Surface fluorescence was also measured continuously for both cruises.

Fluorescence (calibrated as chlorophyll a concentration) ranged from 1µg/L up to 16 µg/L during both G01 and G06 (Figures 11 and 12). The maximums are located directly south of the birdfoot delta as well as southeast of the delta.

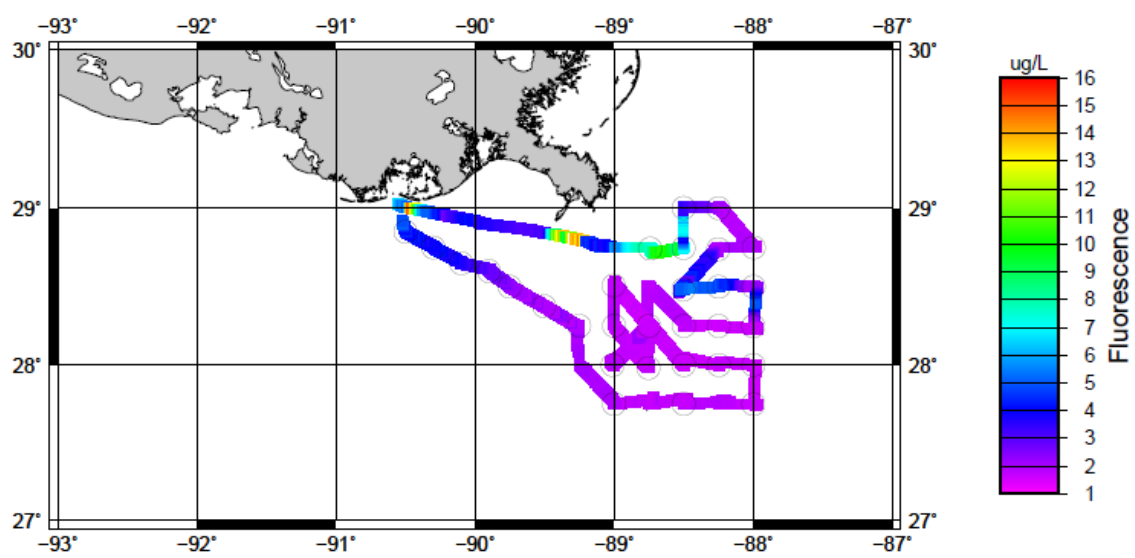


Figure 11. G01 Surface Fluorescence. Fluorescence in $\mu\text{g/L}$ along cruise track. Circles represent stations.

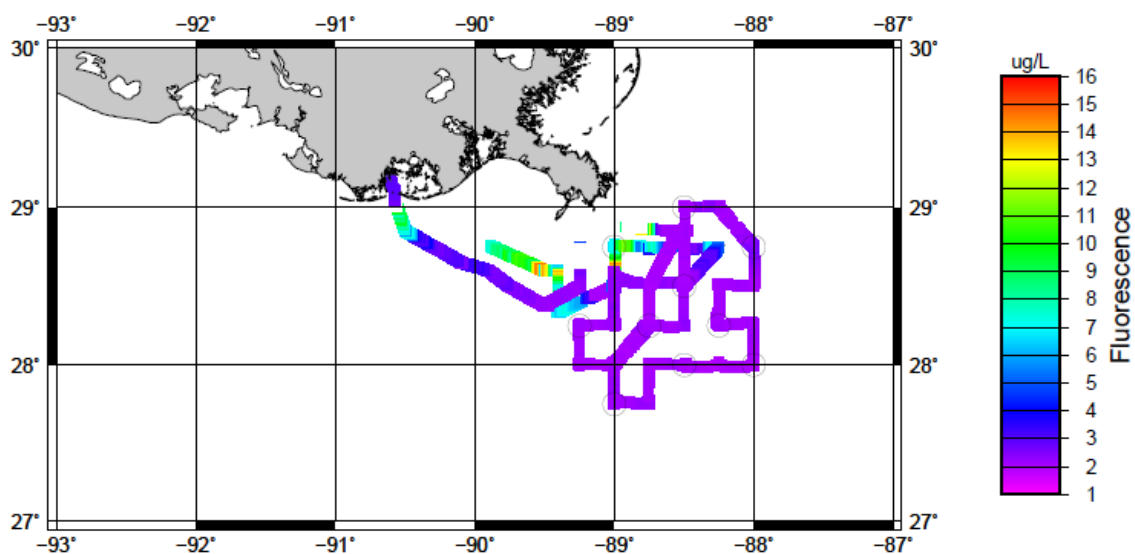


Figure 12. G06 Surface Fluorescence. Fluorescence in $\mu\text{g/L}$ along cruise track. Circles represent stations

DIC surface measurements were taken only on stations. G01 had a maximum surface DIC value of 2259 $\mu\text{mol/kg}$ at the most southern central station and a minimum of 1940 $\mu\text{mol/kg}$ at the farthest southeast station (Figure 13). G06 had a maximum DIC of 2280 $\mu\text{mol/kg}$ located in the middle of the station grid and a minimum of 1834 $\mu\text{mol/kg}$ unexpectedly close to the birdfoot delta (Figure 14).

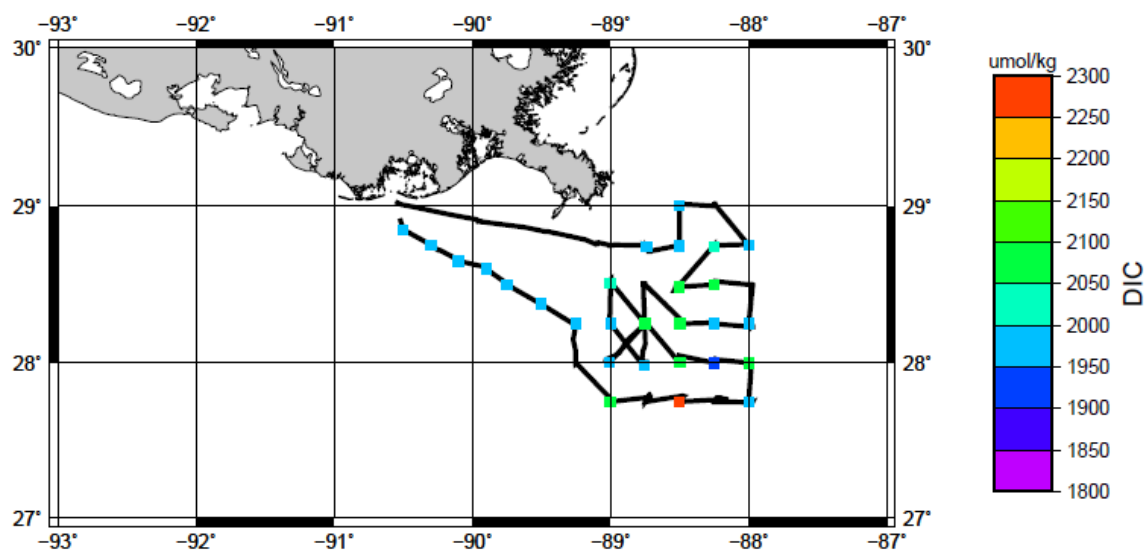


Figure 13. G01 Surface DIC. DIC in $\mu\text{mol/kg}$ along cruise track.

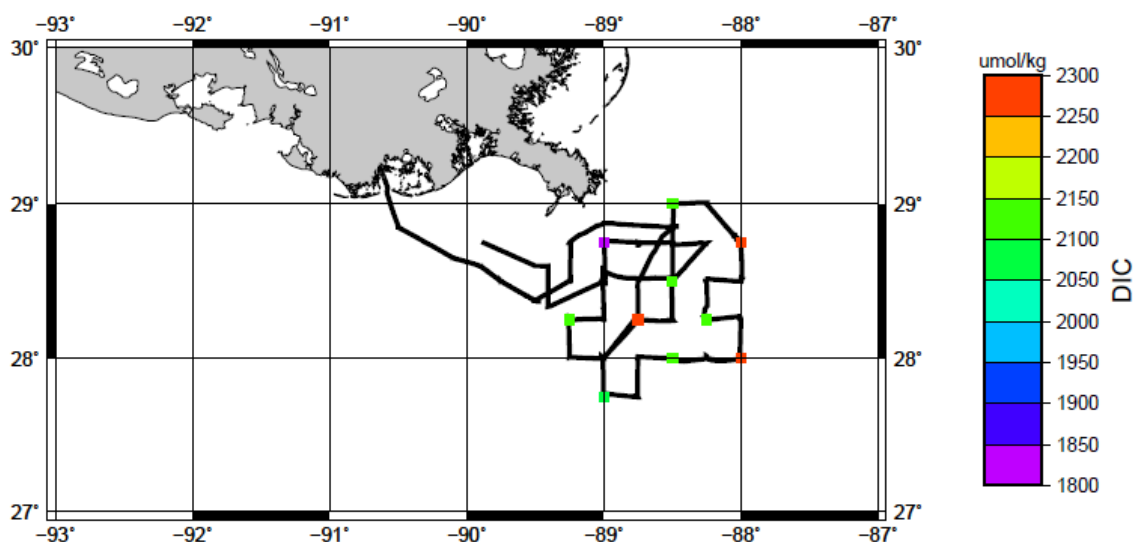


Figure 14. G06 Surface DIC. DIC in $\mu\text{mol/kg}$ along cruise track.

TA was also sampled only on stations throughout the cruise. The surface TA for G01 had a range of 2243 $\mu\text{mol/kg}$ to 1909 $\mu\text{mol/kg}$, with the maximum being found along a diagonal to the southeast of the delta and the minimum found in the Mississippi canyon stations directly south of the delta (Figure 15). G06 showed a maximum TA of 2414 $\mu\text{mol/kg}$ at the northern most station and a minimum TA of 2298 $\mu\text{mol/kg}$ at the station located closest to the delta (Figure 16).

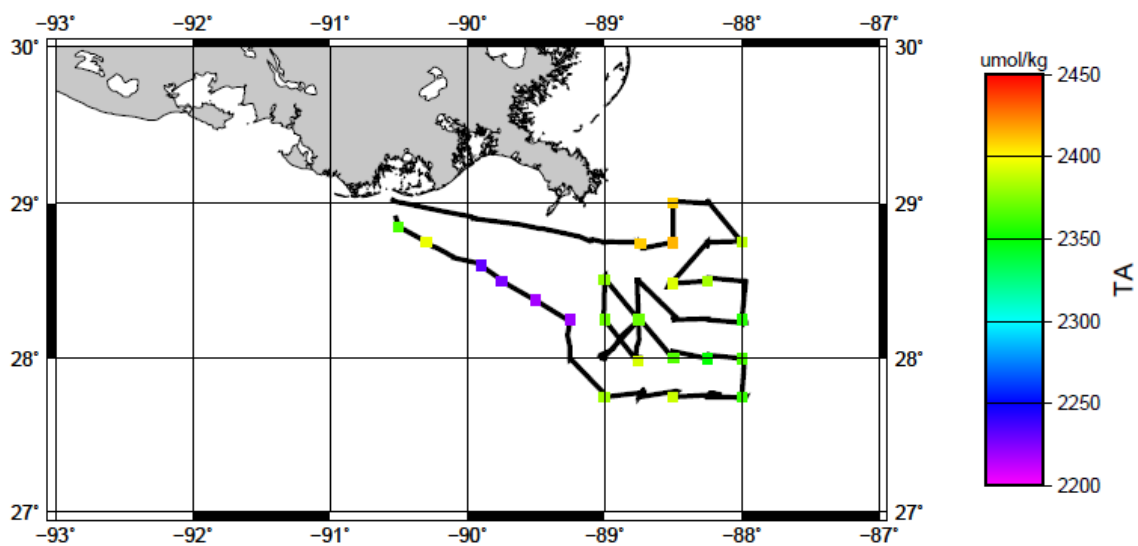


Figure 15. G01 Surface TA. TA in $\mu\text{mol/kg}$ along cruise track, black line represents cruise track.

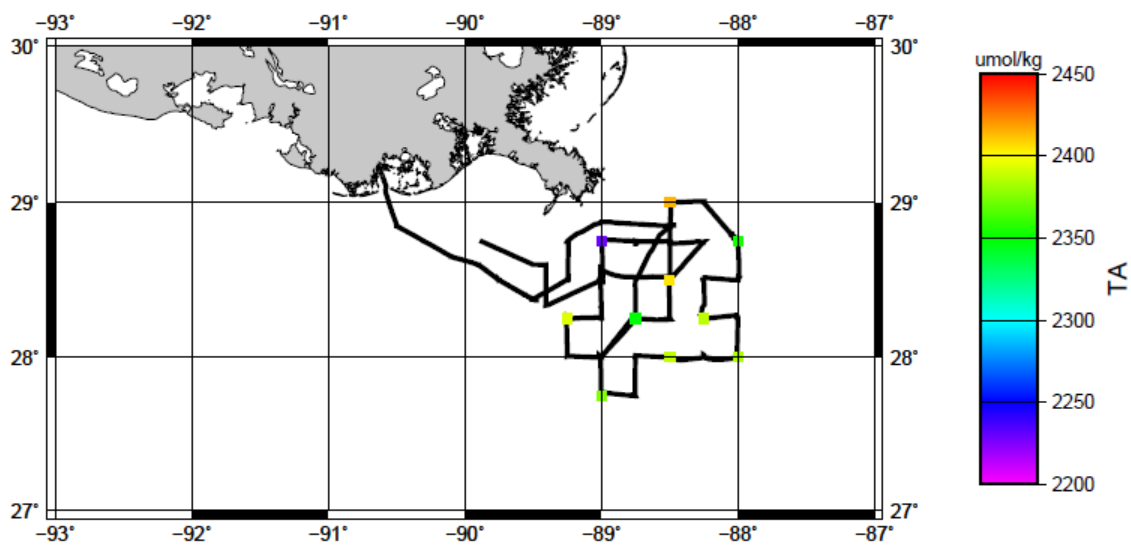


Figure 16. G06 Surface TA. TA in $\mu\text{mol/kg}$ along cruise track, black line represents cruise track.

Calculated saturation states for both calcium and aragonite were calculated for both cruises. Surface values for Ω_{CA} ranged from 2.73 to 8.43 during G01. The maximum was found nearest the birdfoot delta and the minimum was found at the southern most central station (Figure 17). G01's Ω_{ARG} maximum and minimum values were found at the same stations, however the values instead ranged from 1.83 to 5.59. G06 showed a range of Ω_{CA} that was from 1.86 to 6.51. The maximum was located at the station closest to the Mississippi and the minimum at the station southeast of the maximum (Figure 19). The Ω_{ARG} for G06 ranged from 1.24 to 4.35, with the maximum and minimum locations being the same as those of Ω_{CA} (Figure 20).

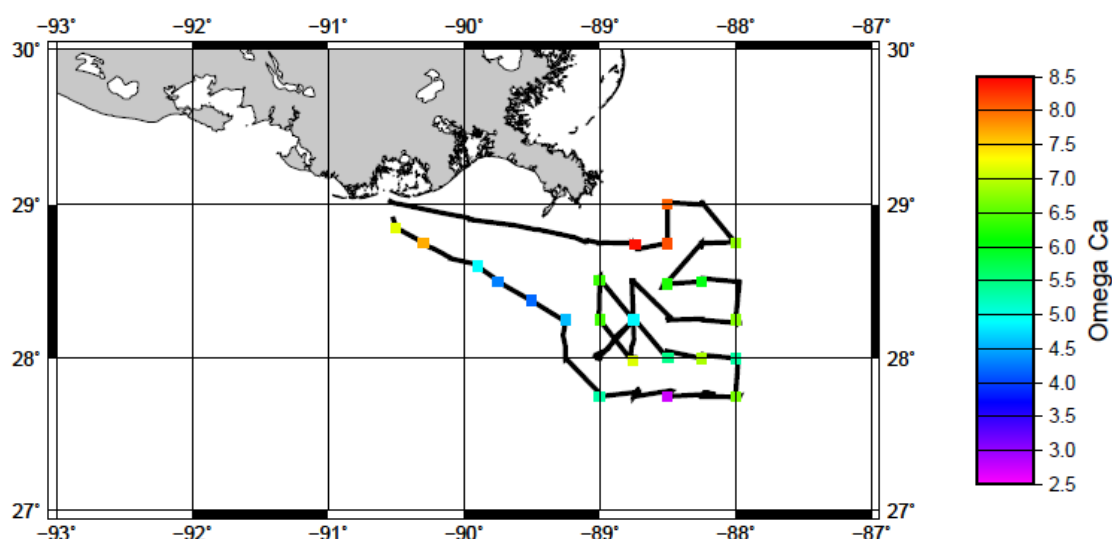


Figure 17. G01 Surface Ω_{CA} . Ω_{CA} along cruise track, black line represents cruise track.

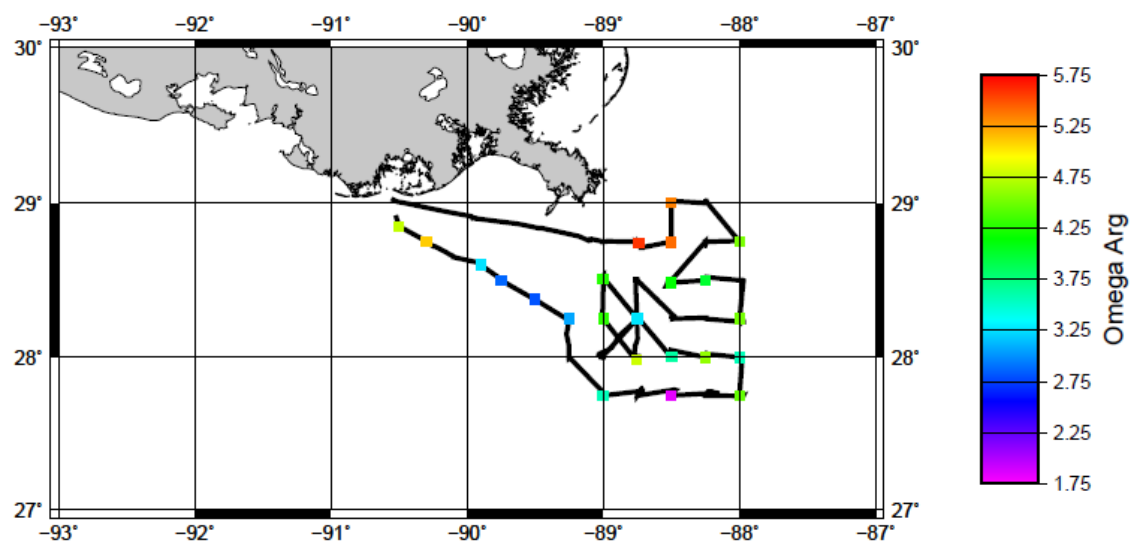


Figure 18. G01 Surface Ω_{ARG} . Ω_{ARG} along cruise track, black line represents cruise track.

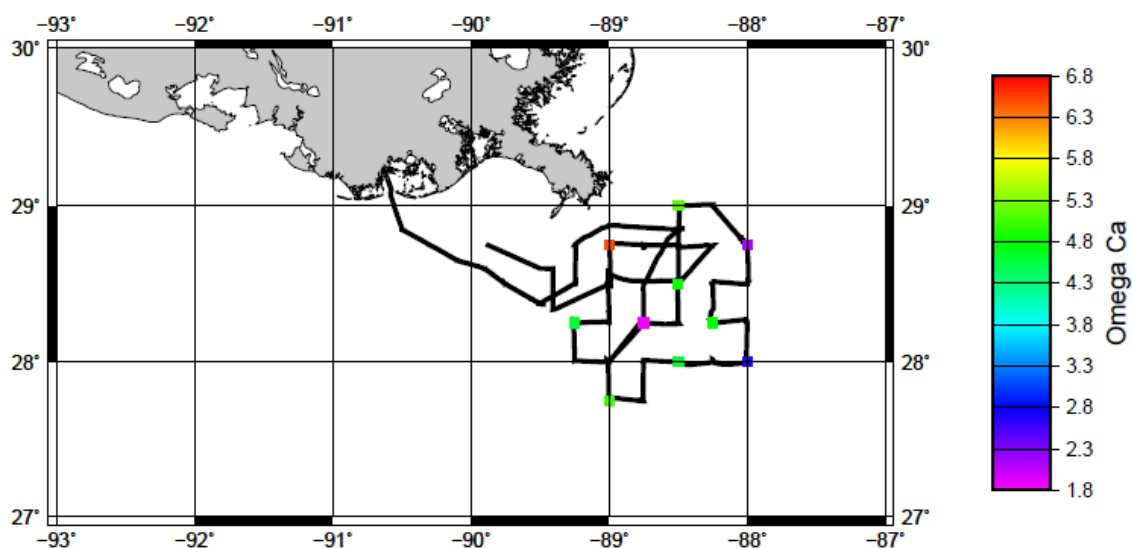


Figure 19. G06 Surface Ω_{CA} . Ω_{CA} along cruise track, black line represents cruise track.

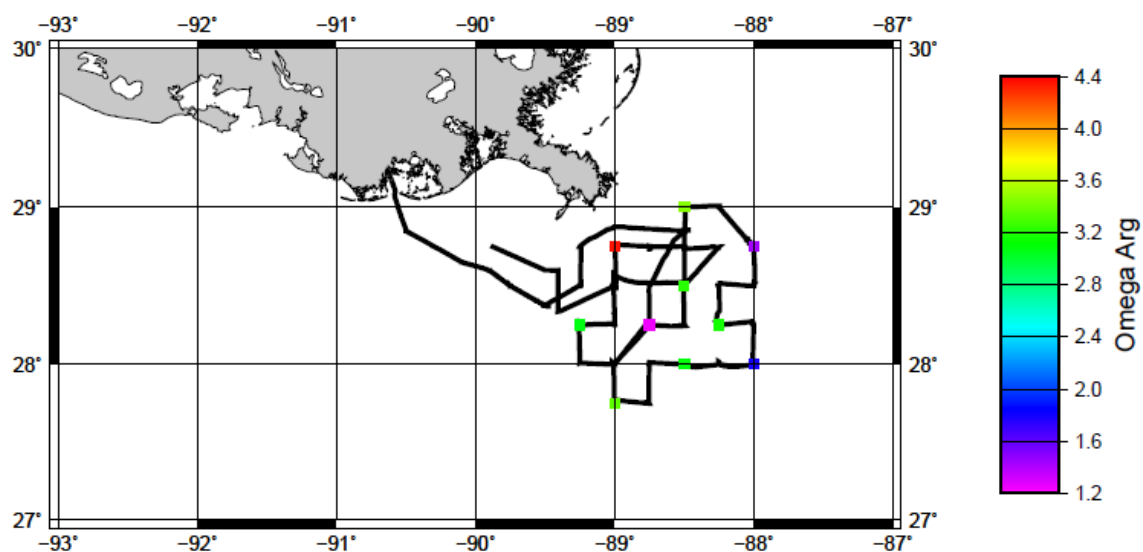


Figure 20. G06 Surface Ω_{ARG} . Ω_{ARG} along cruise track, black line represents cruise track.

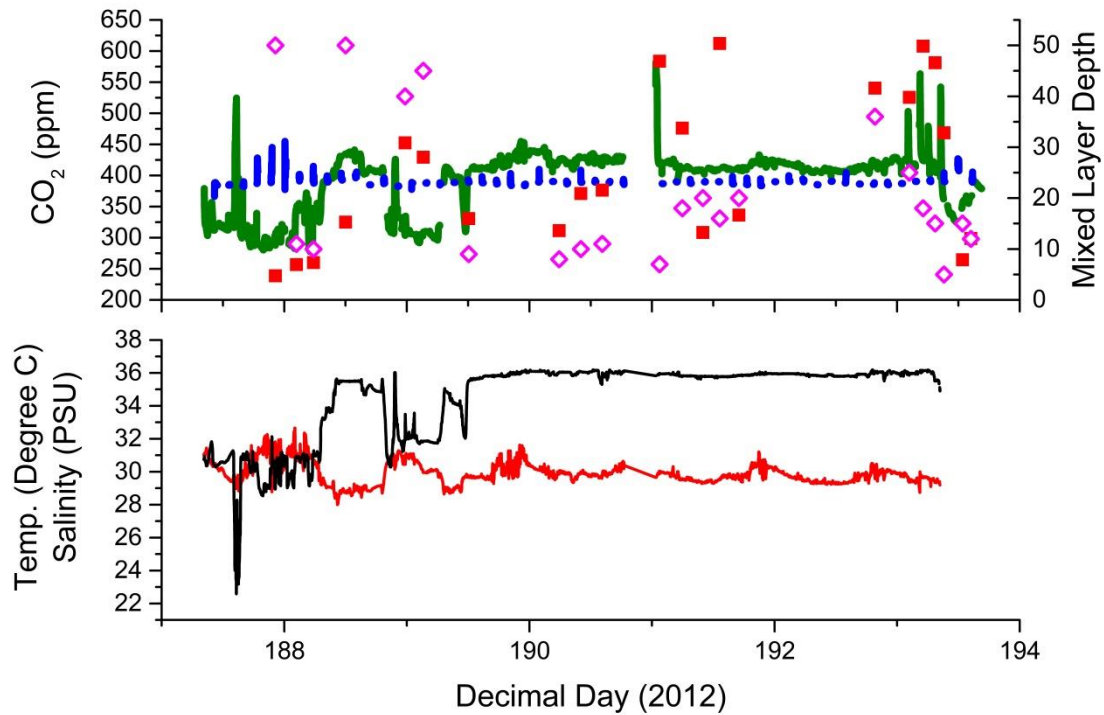


Figure 21. G01 Surface characteristics. In the upper plot, | represents the air pCO₂ values, | represents the surface water pCO₂, bottle calculated values (■) and mixed layer depth (◇). In the bottom graph — represents salinity and — represents temperature.

G01 provided a comprehensive view of the surface waters through use of the bottle values as well as the continuous measurements (Figure 21). G01 had an average of 391 ± 48 ppm surface water pCO₂. In the beginning of the cruise, the pCO₂ values were ~ 100 ppm lower than average, dropping as low as 250 ppm, which explains the large standard deviation. There is also a spike in pCO₂ with an accompanying drop in salinity. This effect is most likely riverine (lower salinity) in origin based on the higher

pCO₂, whereas for the rest of the cruise pCO₂ spikes correlate directly with salinity spikes indicating precipitation and evaporation. The temperature has a negative relationship with pCO₂, which is expected as gas solubility increases with decreasing temperature.

G06 also showed the much lower salinity spikes (~20 PSU) from the average of 36 PSU very early on in the cruise (Figure 22). This is again most likely the riverine input as it occurs again on re-entry to port.

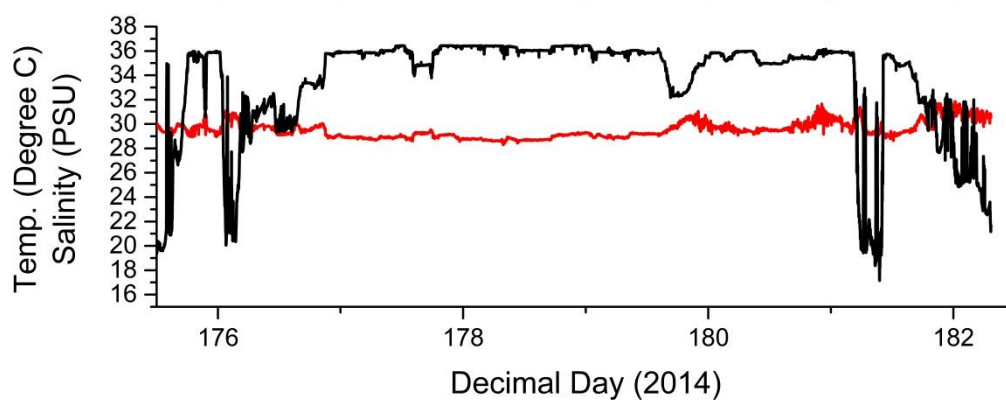


Figure 22. G06 Surface Temperature and Salinity. In the graph — represents salinity and — represents temperature.

3.1 Profile Results

The entirety of the water column was also analyzed and to separate these results from the surface values they will be called “deepwater results” even though they contain the surface values, as well. To allow for a better comparison of the water masses, TA and DIC were normalized to a salinity of 35 and plotted versus density (Figures 23 and 24). The density σ_T is the potential density anomaly, which is calculated by first using temperature and conductivity from the CTD to calculate salinity and using that salinity with potential temperature to calculate the density. The deepwater in the Gulf of Mexico enters via the Yucatan Strait sill at ~2000m depth from the Caribbean Sea (and also exits side by side in this same region). However, data from this area does not exist. CLIVAR line A05 was chosen for comparison as it was the closest major data point to the water entering the Gulf of Mexico and will still represent the North Atlantic Deepwater that would be entering (Figure 25).

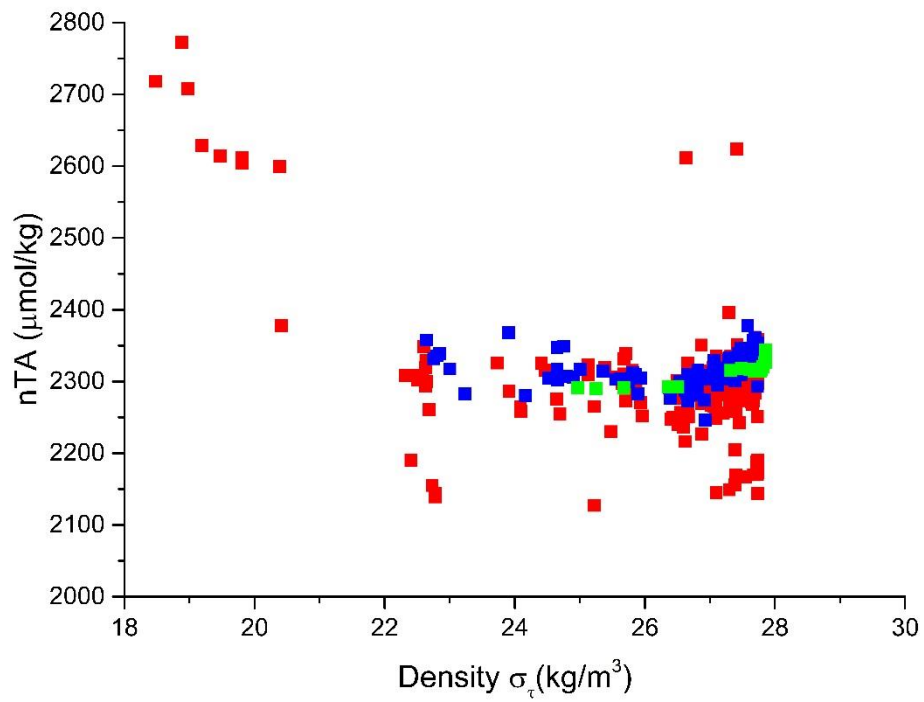


Figure 23. Normalized TA. ■ represents the G01 data, ■ represents the G06 data, and ■ represents the CLIVAR A05 data closest to the Gulf.

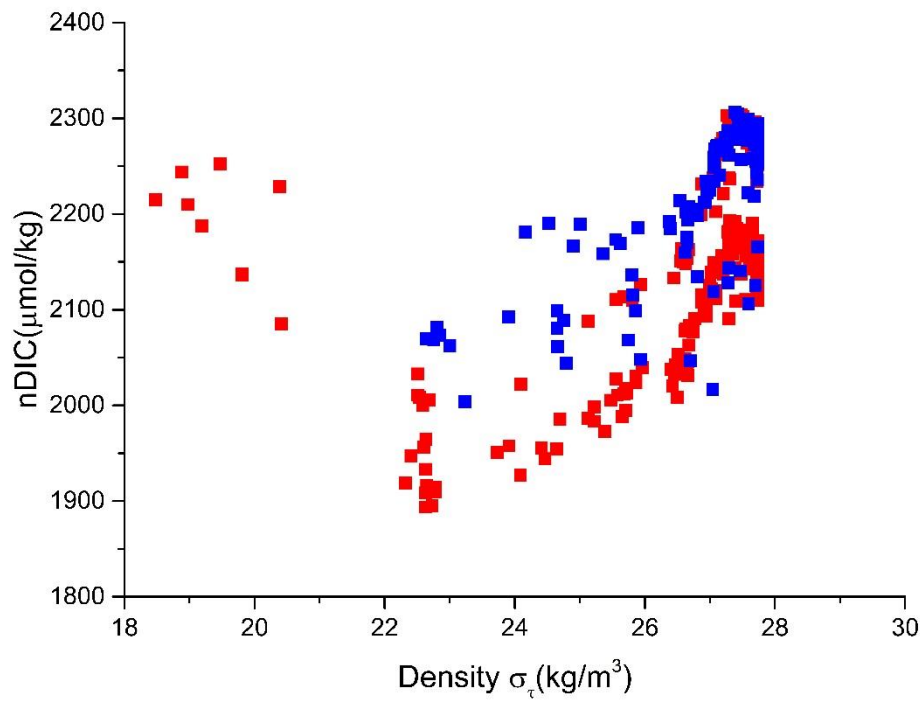


Figure 24. Normalized DIC. ■ represents the G01 data and ■ represents the G06 data.

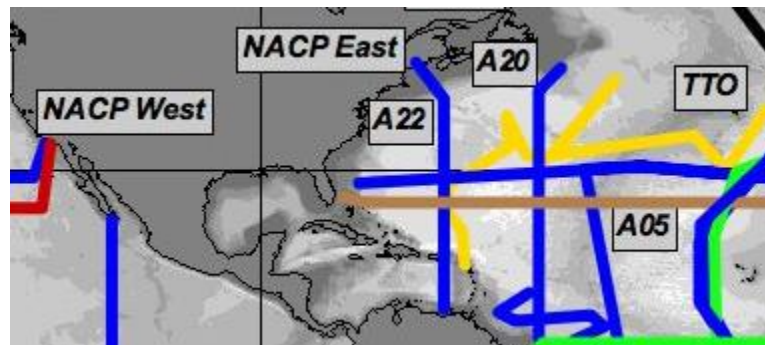


Figure 25. CLIVAR cruise lines. A05 is the line chosen for comparison, shown in brown. [CDIAC, 2015]

Calculated saturation states of both calcite and aragonite are were also plotted against density and showed a maximum of 8.5 and 5.9 for Ω_{CA} and Ω_{ARG} and minimums of 0.65 and 0.42, respectively (Figure 26).

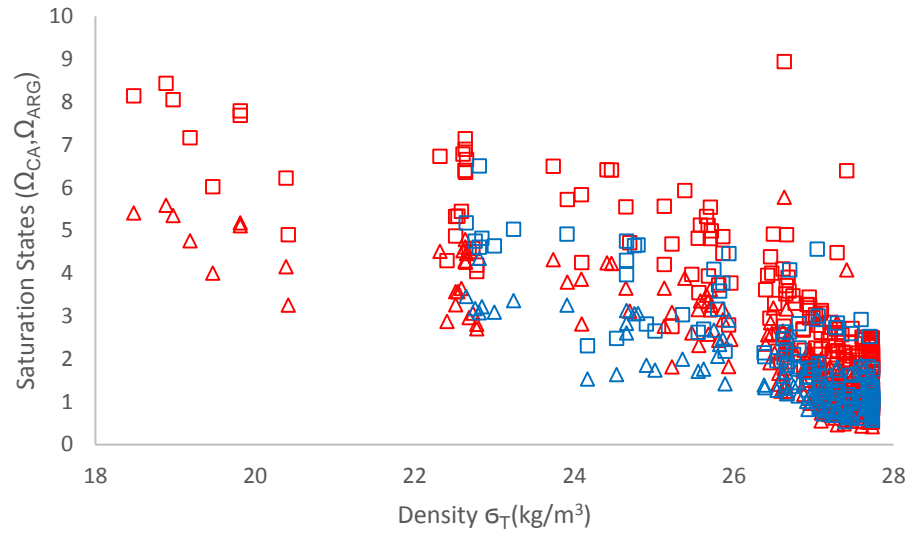


Figure 26. Saturation States. \square represents the G01 Ω_{CA} , \triangle represents the G01 Ω_{ARG} , \square represents the G06 Ω_{CA} , \triangle represents the G06 Ω_{ARG} .

4 DISCUSSION

The Gulf of Mexico is a complicated region of study, especially in the vicinity of the mouths of the Mississippi and Atchafalaya rivers. This water changes direction and extends different distances across the gulf under a variety of circumstance. Surface currents are affected by the loop current and eddies that form from it. Surface carbonate chemistry can be vastly different from the background if affected by these freshwater sources.

The loop current position must be determined to help understand any extra variables of different waters on sampled stations. The loop current can be found not directly affecting any sampled stations from either G01 or G06 (Figures 27 and 28) although the current acts differently for each cruise. During G01, an eddy can be seen already separated from the loop current and travelling closer towards the sampling area; whereas the eddy hadn't fully broken away from the loop current during the G06 cruise. The surface currents flow in different directions at the southerly stations during each cruise, with G01 experiencing an easterly flow and G06 experiencing a westerly flow.

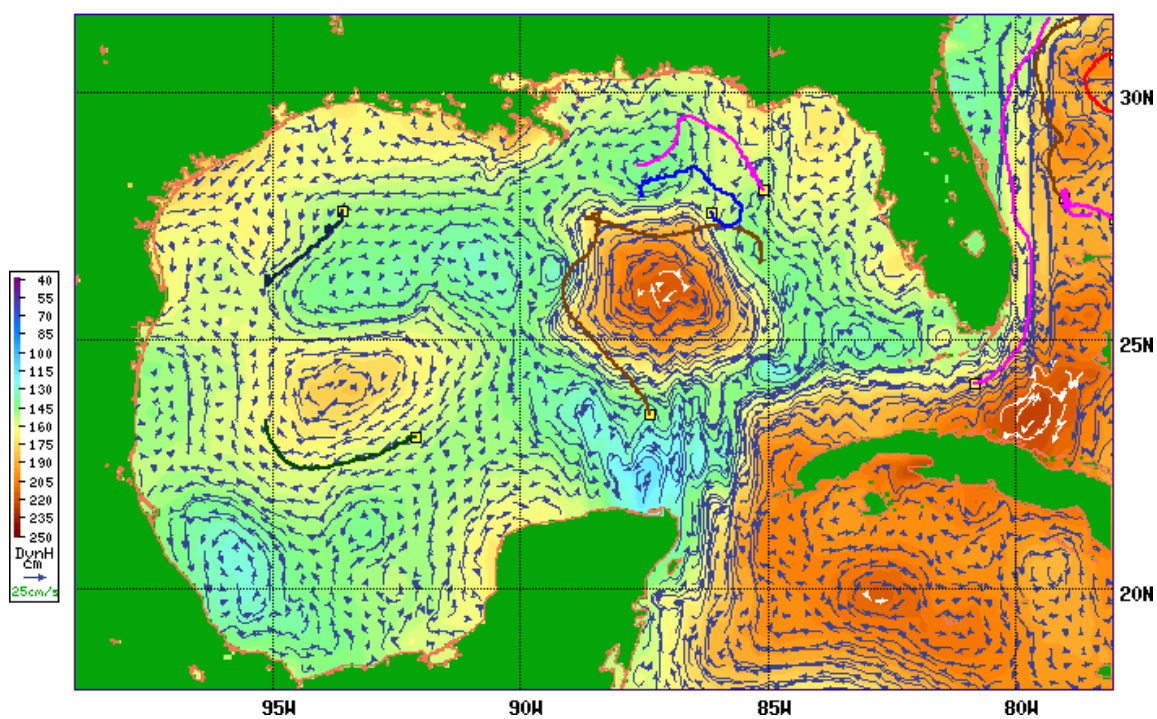


Figure 27. Geostrophic Flows during G01 Cruise.

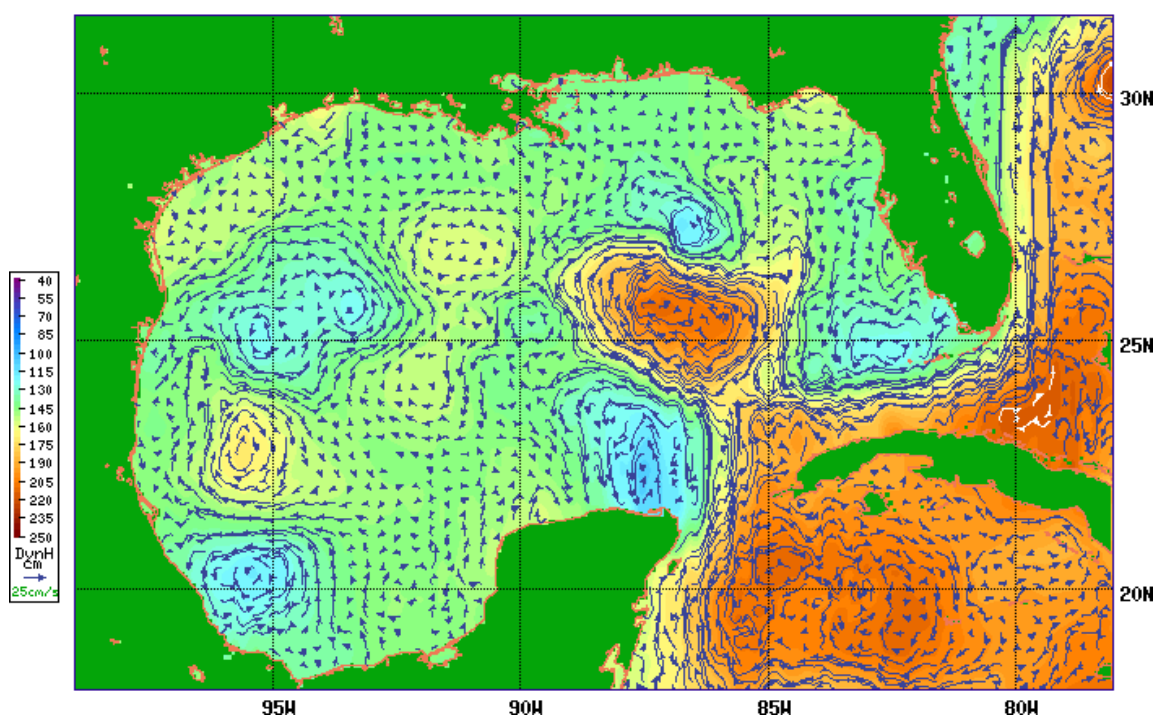


Figure 28. Geostrophic Flows during G06 Cruise.

The freshwater input from the Mississippi can extend outward and affect the chemistry of the surface water in the study region. This process is measured by using conservative characteristics such as salinity, alkalinity, and the non-conservative chlorophyll (fluorescence in this case). This signal can be seen quite strongly in both the G01 and G06 cruises as a tongue of fresher water reaching south from the birdfoot delta (Figures 4 and 6). During G01, this tongue appears to be strongest directly south of the delta with a signal also extending southeast through the sample region (Figure 4). During G06, the effect of freshwater input can be seen through much lower values of salinity, alkalinity and chlorophyll in the same regions, however it appears the salinity is much lower (19 PSU) in the southeast tongue (Figure 6). This means that even though these cruises were roughly at the same time of year, the Mississippi river influence is not seasonally identical in the region. The Mississippi River discharge rate varied drastically between the two cruises with G01 showing an average of 179004 ft³/s and G06 having an average discharge rate of 585358 ft³/s, an increase in flow of about 227% [USGS 2012].

With the water masses characterized, the carbonate system can be assessed. DIC results for G01 showed a centralized plume of higher values, ranging between 2100-2150 µmol/kg while the surrounding values on the northern edge and western canyon were on average ~2000 µmol/kg or below (Figure 13). The higher values are more likely to be the normal open gulf values where photosynthesis is low due to lack

of nutrients, while the lower values at the surrounding stations are most likely due to increased photosynthesis as dissolved CO_2 is used. The increased photosynthesis would be due to the nutrient load coming from the Mississippi River as it interacts with seawater. This agrees with the high fluorescence values and low $\text{pCO}_{2(\text{w})}$ observed at these stations (Figures 7 and 11). The salinity of the water is also much lower in this tongue of fresher river water with values closer to 30 ppm while the open ocean values are consistently ~ 35 ppm. Using an ANOVA analysis of these suggested plume stations versus non plume station with an alpha value of 0.05, the P-value is 0.039. This suggests that the plume stations are statistically different than the rest of the stations and that the Mississippi River is affecting water chemistry significantly. Alkalinity for G01 on the other hand shows a P-value of 0.09 which would say that the alkalinity is not statistically different for these two groups. G06 shows a similar situation with the plume but the number of stations in that region is not high enough to make a statistically significant conclusion. With all of the other parameters established, the saturation states also show a trend in the surface stations. As expected, the saturation states are higher in the region in which the Mississippi River tongue exists. This is due to the Mississippi River providing nutrients that create a high rate of photosynthesis in the area that lowers the DIC concentration. The saturation states are more variable than the individual variables (DIC, TA, Sal etc.). Using a t-test with assumed unequal variances, the relationship between G01 and G06 is statistically significant ($p=0.0025$

for both saturation states). While the saturation states are a function of the other parameters, the relationships are not all linear or additive.

Prior cruises that have been completed in the Gulf of Mexico near the Mississippi River mouth can provide a point of comparison for surface values. The cruises chosen for comparison are GOMECC1 (Gulf of Mexico and East Coast Carbon 1, 2007) and GOMECC2 (Gulf of Mexico and East Coast Carbon 1, 2012) due to their proximity of the region of study as well as their proximity to the mouth of the

Mississippi River. Only one transect of both of these studies (stations off Louisiana) is applicable in this case (Figure 29).

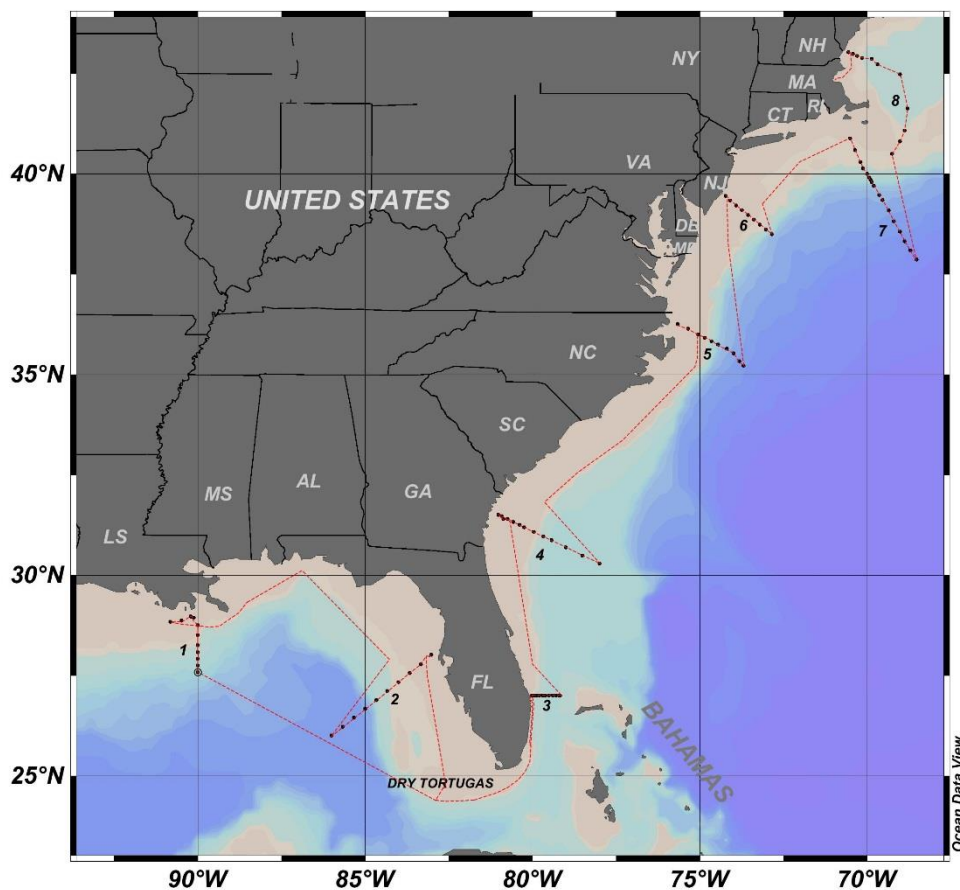


Figure 29. GOMECC2 Cruise Stations. [AOML, 2012]

GOMECC1 shows a lower DIC value in the very low salinity waters, with a DIC of $\sim 1864 \mu\text{mol/kg}$ at ~ 25 salinity. The DIC of much of the lower salinity values (30-32) for G01 show a similar trend in lower values ($1950\text{--}1967 \mu\text{mol/kg}$). However, G06 has very few low salinity stations and appears to show high values of DIC ($2272 \mu\text{mol/kg}$).

GOMECC2 shows rather stable DIC values all around the 2020 $\mu\text{mol/kg}$ average but the range of salinities is limited between 32-36 PSU. GOMECC2 shows the same trend in TA as was in DIC, a rather stable set of values averaging around 2370 $\mu\text{mol/kg}$, once again the salinities measured are also all in the range of 32-36 PSU. GOMECC1 also shows the same expected trend, a lower TA at the very low salinities (TA of $\sim 2317 \mu\text{mol/kg}$ at ~ 25 salinity). However, G01 shows an interesting trend as the lower salinities (30-31 PSU) have a relatively high TA (2400-2420 $\mu\text{mol/kg}$). This appears to be in line with the next point taken via GOMECC1, which shows a TA of 2432 $\mu\text{mol/kg}$ at 31.75 PSU. The values of G01 and G06 appear about as variable as those of GOMECC1 in the higher salinity range (35-36 PSU). A t-test shows that G01 and G06 DIC values are statistically different ($p_{\text{DIC}}=0.0035$) but the relationship between the GOMECC 1 and 2 DIC values aren't statistically significant ($p_{\text{DIC}}=0.234$). As for the TA, G01 and G06 aren't statistically different ($p_{\text{TA}}=0.188$) while the TA values between the GOMECC cruises are statistically different ($p_{\text{TA}}=0.0178$). This suggests that DIC values varied more during the GOMECC cruises than GISR and TA values varied more during the GISR cruises than GOMECC. When comparing G01 to the GOMECC cruises; G01 show significant difference between TA but not DIC with GOMECC 1 ($p_{\text{TA}}=0.008$, $p_{\text{DIC}}=0.124$) and statistical difference between both TA and DIC for GOMECC 2 ($p_{\text{TA}}=0.051$, $p_{\text{DIC}}=0.005$). Looking at G02 next to the GOMECC cruises, G02 shows no significant difference between TA, however the DIC is significantly different during GOMECC 1 ($p_{\text{TA}}=0.1560$, $p_{\text{DIC}}=.006$) and the same for GOMECC 2 ($p_{\text{TA}}=0.404$, $p_{\text{DIC}}=0.009$). This

comparison suggests the variability the northern Gulf of Mexico exists in other similar carbonate studies, and that the variability in the GISR cruises is comparable to that of GOMECC's cruises. This also suggests that any affect the Deepwater Horizon spill had on the carbonate system is likely not existing anymore.

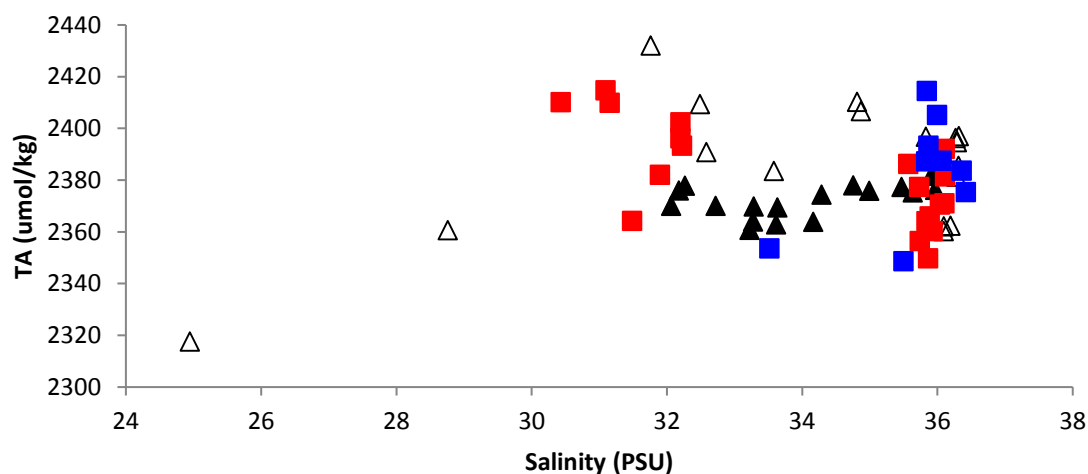
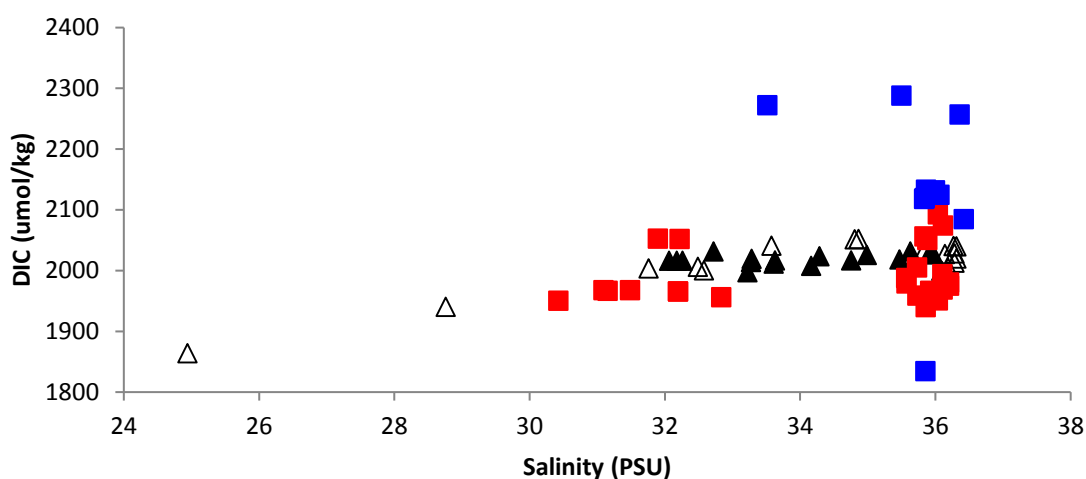


Figure 30. GISR versus GOMECC TA Comparison. Δ represents the GOMECC1, \blacktriangle represents GOMECC2, \blacksquare represents G01, \blacksquare and represents G06.



residence time of deep water in the Gulf of Mexico is short enough that the alkalinity values will likely stay comparable to those entering the gulf via the Yucatan Strait. Or it is possible that the deepwater measured in this region has entered the Gulf of Mexico very recently and hasn't travelled around the gulf for a possibility to see any changes yet. Saturation states versus density show that both G01 and G06 drop rapidly with depth (Figure 26). These saturation states approach an average of one at the most dense waters. The saturation states can be used as a proxy for understanding ocean acidification as they are derived from the values of the entire carbonate system. Thus with only the densest waters (depths greater than 500 meters) reaching the value of 1 or lower (cold salty deepwater with higher DIC due to respiration) it can be assumed that the waters in the study region were favorable for organisms that would use calcite or aragonite for their structures, strictly speaking in relation to the carbonate system. As for future analysis, these values could be compared to find if ocean acidification is taking place (the saturation states would likely drop slightly nearer the surface waters).

5 CONCLUSIONS AND FUTURE WORK

5.1 Conclusions

Prior to this study, the understanding of the carbonate system for this area was limited. Utilizing two separate years of data in an overlapping region it was conclusive that the surface carbonate chemistry is changed due to riverine input, as expected. The Mississippi River lowers the surface salinity (19 PSU from 36 PSU average) and TA (2200 $\mu\text{mol/kg}$ from ~ 2350 $\mu\text{mol/kg}$ average) while indirectly lowering the DIC (to 1800 $\mu\text{mol/kg}$ from ~ 2000 $\mu\text{mol/kg}$ average) due to nutrient input and thus photosynthesis. This area of freshened water is not seasonally identical year to year, likely due to precipitation leading to different Mississippi River discharge rates (227% higher in 2014 than in 2012) and surface wind patterns.

Surface DIC and TA measurements showed varied significance to that of other cruises in the region, the GOMECC 1 and 2 cruises. This comparison also showed that statistical significance existed not only between the comparison cruise sets, but also within the repeat cruises. Although TA values changed with riverine input between the GISR cruises, the variance wasn't enough to make them statistically different. However, the DIC between the cruises was statistically significant and this is likely due to the amount of nutrients brought in with the differing discharge rates.

The contribution of ocean acidification to the saturation states of this region are muted by the Mississippi River influence. The low levels of total alkalinity along with the high nutrients to create low DIC values from the riverine input create much larger values for aragonite and calcite saturation states than the decrease in saturation states the estimated few ppm per year increase in atmospheric carbon dioxide would cause as it dissolved into surface waters (if $p\text{CO}_2$ increases 2ppm both saturation states decrease roughly 0.01). With saturation states only reaching the unfavorable states (1 or below) at the most dense waters during sampling, values favored calcite and aragonite structure builders. To measure ocean acidification in the region, data could serve as a baseline for comparison for future ocean acidification research as anthropogenic atmospheric CO_2 increases. Although a larger (and more frequent) region of study to measure Mississippi River plume influence would be needed. Understanding the variability observed in this region requires having more stations covering more times of year as flow rates of freshwater input change.

The deepwater total alkalinity of the northern Gulf of Mexico shows similar values to that of the Atlantic Ocean CLIVAR cruise station AO5. The CLIVAR station showed a salinity normalized TA value of $\sim 2300 \mu\text{mol/kg}$, which was within the standard deviation of G01 and G06 at densities between 24 and 28 kg/m^3 . Low density values for both TA and DIC are variable, once again due to the Mississippi River influence as low density implies fresher surface water. This suggests that the

deepwater in the Gulf of Mexico is comparable to that of the deepwater outside of the gulf, and also suggests that post spill deepwater is similar to the pre spill deepwater.

5.2 Future Work

Establishing a baseline for the Gulf of Mexico is important because now more measurements can be made to determine change from this point on as there are very few that cross this region. The study of the two GISR cruises G01 and G06 lead to some interesting questions such as how the DIC and TA can affect the pH of waters around the Gulf of Mexico and whether that water mass will carry these signatures over distance or dilute them through mixing. More future work that would be beneficial is to establish the pH values of the deep water entering and exiting the Gulf of Mexico at the Yucatan Strait to help understand if the gulf is contributing enough respiration of hydrocarbons to affect the water mass' acidity. To do this, more work would need to be done sampling at the Yucatan sill at depths of around 2040 meters and over multiple years to establish a temporal knowledge of the system.

Better spatial coverage would also allow for a more balanced understanding of the deep waters of the Gulf of Mexico. There have been more GISR cruises (G05) that cover a larger portion of the gulf that could help build a foundation such as this due to the samples in Mexican owned waters. However, the quantity of samples was minimal due to bottles available. Knowing the pH of the waters around the major ecosystems such as the Flower Gardens National Bank could help in case of other major oil spills or

accidents in the gulf that could possibly happen due to the sheer number of rigs in place. Since it is established that the water in the gulf does not stagnate around a given area for very long, knowing how the DIC is increased in distinct areas before an event such as a spill occurs will help predict pH decreases and may give initial warnings to communities that support a large portion to gulf economies (such as oyster beds).

To obtain a better understanding of how the surface waters change, a long term study would be needed. This study would have to have a better spatial coverage as well as more intervals of time, such as once or twice a year measurements. This would allow for a better average to be found on a seasonal scale that would be more characteristic of the normal parameters.

Lastly, determining the deep water variability for the dissolved inorganic carbon would be interesting. This would explain whether certain regions are prone to more respiration and how far that increase in DIC would affect surrounding waters. With the numerous seeps in the gulf, sampling either close to the origin of hydrocarbons or definitively far from a seep would help show the overall effect of this oil degradation on the community. Also, modeling the flow of this water if it was a lower pH would help show how quickly it leaves the starting area before it either moves on or is diluted through mixing.

REFERENCES

AOML (Atlantic Oceanographic and Meteorological Laboratory) (2012)
<http://www.aoml.noaa.gov/ocd/gcc/GOMECC2/>

CDIAC (Carbon Dioxide Information Analysis Center) (2015)
<http://cdiac.ornl.gov/oceans/RepeatSections/>

Caldeira K. and M.E. Wickett (2005), Ocean model predictions of chemistry changes from carbon dioxide emissions to the atmosphere and ocean, *Journal of Geophysical Research*, Vol. 110, Issue C9

Dickson, A. G., C. L. Sabine, and J. R. Christian (eds.) (2007), Guide to best practices for ocean CO₂ measurements, in *PICES Special Publication 3*, p. 191.

Doney, S.C., W.M. Balch, V.J. Fabry, and R.A. Feely, (2009), Ocean Acidification: A Critical Emerging Problem for the Ocean Sciences, *Oceanography*, Vol. 22, no. 4, pp 16-25

EPA General Facts (2012) <http://www.epa.gov/gmpo/about/facts.html>

Kvenvolden, K.A., and C.K. Cooper (2003) Natural seepage of crude oil into the marine environment, *Geomarine letters*, Vol. 23, Issue 3-4, pp 140-146

Le Quéré, C., T. Takahashi, E. T. Buitenhuis, C. Roedenbeck, and S. C. Sutherland, (2010) Impact of climate change and variability on the global oceanic sink of CO₂. *Global Biogeochem. Cycles*, 24, Gb4007.

Nowlin, W. D., A.E. Jochens, S. F. DiMarco, R. O. Reid, and M.K. Howard (2001), *Deepwater Physical Oceanography Reanalysis and Synthesis of Historical Data*. U.S. Department of the Interior Minerals Management Service.

Orr, J.C., V. J. Fabry, O. Aumont, L. Bopp, et al. (2005) Anthropogenic ocean acidification over the twenty-first century and its impact on calcifying organisms, *Nature*, Issue 437, pp 681-686.

Pierrot, D., C. Niell, K. Sullivan, R. Castle, R. Wanninkhof, H. Lüger, T. Johannessen, A. Olsen, R. A. Feely, and C. E. Cosca (2009), Recommendations for autonomous underway pCO₂ measuring systems and data-reduction routines, *Deep Sea Research II: Topical Studies in Oceanography*, 56(8), pp 512-522.

Pierrot, D., E. Lewis, and D. W. R. Wallace. 2006. MS Excel program developed for CO₂ system calculations. Carbon Dioxide Information Analysis Center, Oak Ridge National CO₂ system along U.S. Atlantic coast 341 Laboratory. Oak Ridge, Tennessee. ORNL/CDIAC-105a, U. S. Department of Energy, doi:10.3334/CDIAC/otg.CO2SYS_XLS_CDIAC105a

Sabine, C.L., R.A. Feely, N. Gruber, R.M. Key et al. (2004) The Oceanic sink for Anthropogenic CO₂, *Science*, Vol. 305, Issue 5682, pp 367-371 Princeton, Woodstock: Princeton University Press.

Seibel, B.A. and P.J. Walsh (2001) Potential impacts of CO₂ injection on deep-sea biota, *Science* 12 v.294 no.5541 pp 319-320

Takahashi, T. (1961), Carbon Dioxide in the atmosphere and in Atlantic Ocean Water, *Journal of Geophysical Research*, 66(2), pp 477-494

Tans, P., (2009), An accounting of the observed increase in oceanic and atmospheric CO₂ and an outlook for the future. *Oceanography*, 26–35.

U.S. Geological Survey (USGS), 2012, National Water Information System data available on the World Wide Web (USGS Water Data for the Nation), accessed [January, 2016], at URL [<http://waterdata.usgs.gov/nwis/>]

Wang, Z.A., R. Wanninkhof, W.J. Cai, R.H. Byrne, X. Hu, T.H. Peng, and W.J. Huang (2013) The marine inorganic carbon system along the Gulf of Mexico and Atlantic coasts of the United States: Insights from a transregional coastal carbon study, *Limnology and Oceanography*, Vol. 58, pp 325-342

Wanninkhof R., L. Barbero, R. Byrne, W.Cai, W. Huang, J.Zhang, and C. Langdon (2015), Ocean Acidification along the Gulf Coast and East Coast of the USA, *Continental Shelf Research*, Volume 98, pp 54-71